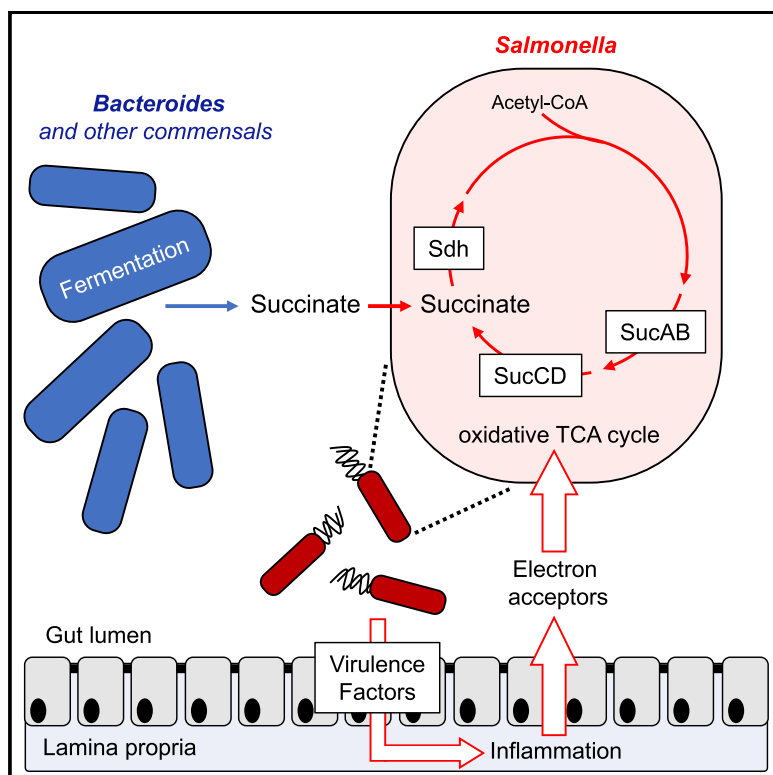


Cell Host & Microbe

An Oxidative Central Metabolism Enables *Salmonella* to Utilize Microbiota-Derived Succinate

Graphical Abstract



Authors

Luisella Spiga, Maria G. Winter,
Tatiane Furtado de Carvalho, ...,
Renato L. Santos, Lora V. Hooper,
Sebastian E. Winter

Correspondence

sebastian.winter@utsouthwestern.edu

In Brief

Spiga et al. show that during colonization of the intestinal lumen, the enteric pathogen *S. Typhimurium* performs a complete TCA cycle. This oxidative central metabolism enables *S. Typhimurium* to utilize the microbiota-derived fermentation product succinate as a nutrient and to compete with the microbiota for colonization of the intestinal tract.

Highlights

- During gut colonization, *S. Typhimurium* performs a complete, oxidative TCA cycle
- Host-derived alternative electron acceptors impact *S. Typhimurium* central metabolism
- Uptake of C4-dicarboxylates enhances *S. Typhimurium* fitness in the inflamed intestine
- Utilization of microbiota-derived succinate supports growth of *S. Typhimurium* in the gut lumen

An Oxidative Central Metabolism Enables *Salmonella* to Utilize Microbiota-Derived Succinate

Luisella Spiga,^{1,9} Maria G. Winter,^{1,9} Tatiane Furtado de Carvalho,² Wenhan Zhu,¹ Elizabeth R. Hughes,¹ Caroline C. Gillis,¹ Cassie L. Behrendt,³ Jiwoong Kim,⁴ Daniela Chessa,⁵ Helene L. Andrews-Polymenis,⁶ Daniel P. Beiting,⁷ Renato L. Santos,² Lora V. Hooper,^{3,8} and Sebastian E. Winter^{1,10,*}

¹Department of Microbiology, UT Southwestern Medical Center, Dallas, TX 75390, USA

²Departamento de Clínica e Cirurgia Veterinárias, Escola de Veterinária, Universidade Federal de Minas Gerais, Belo Horizonte, MG, Brazil

³Department of Immunology, UT Southwestern Medical Center, Dallas, TX 75390, USA

⁴Department of Clinical Science, Quantitative Biomedical Research Center, UT Southwestern Medical Center, Dallas, TX 75390, USA

⁵Department of Biomedical Science, School of Medicine, University of Sassari, Sassari, Italy

⁶Department of Microbial Pathogenesis and Immunology, College of Medicine, Texas A&M University System Health Science Center, Bryan, TX 77807, USA

⁷Department of Pathobiology, School of Veterinary Medicine, University of Pennsylvania, Philadelphia, PA 19104, USA

⁸Howard Hughes Medical Institute, UT Southwestern Medical Center, Dallas, TX 75390, USA

⁹These authors contributed equally

¹⁰Lead Contact

*Correspondence: sebastian.winter@utsouthwestern.edu

<http://dx.doi.org/10.1016/j.chom.2017.07.018>

SUMMARY

The mucosal inflammatory response induced by *Salmonella* serovar Typhimurium creates a favorable niche for this gut pathogen. Conventional wisdom holds that *S. Typhimurium* undergoes an incomplete tricarboxylic acid (TCA) cycle in the anaerobic mammalian gut. One change during *S. Typhimurium*-induced inflammation is the production of oxidized compounds by infiltrating neutrophils. We show that inflammation-derived electron acceptors induce a complete, oxidative TCA cycle in *S. Typhimurium*, allowing the bacteria to compete with the microbiota for colonization. A complete TCA cycle facilitates utilization of the microbiota-derived fermentation product succinate as a carbon source. *S. Typhimurium* succinate utilization genes contribute to efficient colonization in conventionally raised mice, but provide no growth advantage in germ-free mice. Mono-association of gnotobiotic mice with *Bacteroides*, a major succinate producer, restores succinate utilization in *S. Typhimurium*. Thus, oxidative central metabolism enables *S. Typhimurium* to utilize a variety of carbon sources, including microbiota-derived succinate.

INTRODUCTION

The bacterial species dominating the microbiota in the large bowel are obligate anaerobic bacteria belonging to the phyla Bacteroidetes (class Bacteroidia) and Firmicutes (class Clostridia). With amino acids and simple sugars being absorbed in the small intestine, the primary carbon and energy sources for obligate anaerobic bacteria in the large intestine are complex glycans of dietary and host origin (reviewed in Fischbach and

Sonnenburg, 2011; Flint et al., 2012; Koropatkin et al., 2012; Martens et al., 2014). Glycan degradation by the starch utilization system (*sus*) machinery has been studied extensively in obligate anaerobic commensal *Bacteroides* spp. The genomes of sequenced *Bacteroides* strains are predicted to encode a large variety of distinct, *sus*-like systems that allow the utilization of a plethora of structurally unrelated glycans (Cuskin et al., 2015; El Kaoutari et al., 2013; Rogowski et al., 2015; Xu et al., 2003), with different *Bacteroides* strains exhibiting preference for distinct glycans (Pudlo et al., 2015). Similarly, commensal *Bifidobacterium* spp. and *Clostridia* produce extracellular glycoside hydrolases and other carbohydrate-active enzymes, allowing the fermentation of complex polysaccharides (Crost et al., 2013; El Kaoutari et al., 2013; Schell et al., 2002; Schwarz et al., 2004; Shimizu et al., 2002). Glycan degradation by *Clostridia* and *Bacteroidia* generates primary fermentation end products, which support the growth of syntrophic bacteria and archaea as minor constituents of the gut microbiota (Macy et al., 1975; Turton et al., 1983). Collectively, the ability to degrade a variety of complex polysaccharides directly correlates with the overall abundance of commensal gut microbes in the ecosystem (Eilam et al., 2014), indicating that polysaccharide utilization is a major determinant of the microbiota composition in the healthy gut.

Curiously, infection with enteric pathogens disturbs the normal gut microbiota structure, culminating in a bloom of the luminal pathogen population (Barman et al., 2008; Lupp et al., 2007; Stecher et al., 2007). Increased bacterial colonization of the intestinal tract enhances transmission success of the pathogen by the fecal-oral route (Lawley et al., 2008; Rivera-Chavez et al., 2016). Proteobacteria express a very limited number of secreted glycoside hydrolases (El Kaoutari et al., 2013), suggesting that the metabolic pathways that allow gut colonization of pathogenic Enterobacteriaceae such as *Salmonella enterica* serotype Typhimurium (S. Tm; phylum Proteobacteria, family Enterobacteriaceae) must be different from the glycan-foraging mechanisms utilized by commensal Bacteroidia and Clostridia.

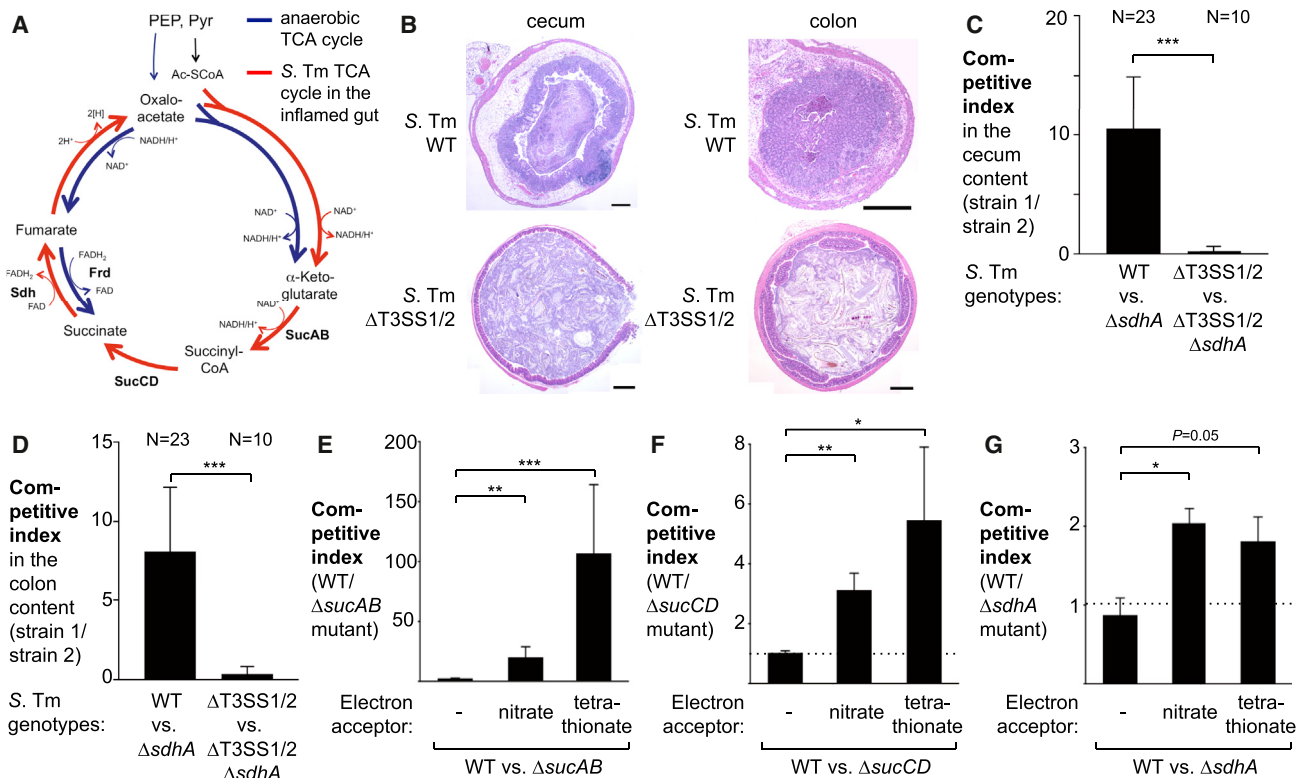


Figure 1. Contribution of Succinate Dehydrogenase to Colonization in the Streptomycin-Treated Mouse Model

(A) Simplified model of the branched *S. Tm* TCA cycle under anaerobic conditions (blue arrows) and complete TCA in the inflamed gut. Frd, fumarate reductase; Sdh, succinate dehydrogenase; SucAB, α-ketoglutarate dehydrogenase; SucCD, succinyl-CoA synthetase.

(B) Streptomycin-pretreated C57BL/6 mice were intragastrically inoculated with the *S. Tm* wild-type (WT) strain or a *ΔinvA ΔspiB* (*ΔT3SS1/2*) mutant. Representative images of H&E-stained sections of the cecum and the colon. Scale bar, 500 μm.

(C and D) Streptomycin-pretreated C57BL/6 mice were intragastrically inoculated with an equal mixture of the indicated *S. Tm* strains. The competitive index in the cecal (C) and colonic content (D) was determined 4 days after infection.

(E–G) Mucin broth was inoculated with an equal mixture of the *S. Tm* wild-type strain (WT) and a *ΔsucAB* mutant (E), a *ΔsucCD* mutant (F), or a *ΔsdhA* mutant (G), and the competitive index determined after 16 hr of anaerobic growth in the absence or presence of nitrate (40 mM) and tetraphionate (40 mM).

Bars represent geometric means, error bars represent the SE. *p < 0.05; **p < 0.01; ***p < 0.001. The number of animals per group (N) is indicated above each bar. See also Figure S1.

Several mechanisms have been shown to enhance fitness of *S. Tm* in the inflamed gut. Modifications of the outer membrane confer resistance to antimicrobial peptides and bile (Crawford et al., 2012; Gunn, 2008). To overcome nutritional immunity, siderophores facilitate the uptake of micronutrients such as iron and zinc (Liu et al., 2012; Raffatellu et al., 2009). By-products of reactive nitrogen and oxygen species generated in the wake of the host inflammatory response are utilized as respiratory electron acceptors (Lopez et al., 2012; Winter et al., 2010). Furthermore, inflammation-associated changes in the colonocyte metabolism include leakage of molecular oxygen into the lumen, which supports oxygen respiration in *S. Tm* through high-affinity terminal oxidases (Rivera-Chavez et al., 2016). Utilization of microbiota-derived molecular hydrogen enhances initial colonization of the intestinal tract by *S. Tm* (Maier et al., 2013). While colonization of the inflamed gut by *S. Tm* has been studied extensively, the adaptation of the central metabolism to the nutritional environment of the inflamed intestine has not been elucidated. Here, we investigated the tricarboxylic acid (TCA) cycle as part of the central intermediary metabolism in the enteric pathogen *S. Tm* in an inbred mouse model of infection.

RESULTS

Contribution of TCA-Cycle Enzymes to Fitness of *S. Tm* in the Streptomycin-Treated Mouse Model

Current dogma holds that Enterobacteriaceae and many other bacteria do not express α-ketoglutarate dehydrogenase (SucAB), succinyl-coenzyme A (CoA) synthetase (SucCD), and succinate dehydrogenase (Sdh) under anaerobic conditions, resulting in a bifurcation of the TCA into a reductive and oxidative branch (Figure 1A) (Amarasingham and Davis, 1965; Cronan and Laporte, 2013; Iuchi and Lin, 1988). In this arrangement, biosynthetic reactions of the TCA cycle can still occur, but acetyl-CoA cannot be fully oxidized. Surplus reduction equivalents are used to reduce the internal terminal electron acceptor fumarate. Based on these considerations, one would assume that the TCA cycle of *S. Tm* in the gut lumen is branched and α-ketoglutarate dehydrogenase, succinyl-CoA synthetase, and Sdh activity is dispensable (Figure 1A). To test this idea, we generated an *S. Tm* mutant lacking the major subunit of Sdh (*ΔsdhA*) and determined fitness in a murine model of *Salmonella*-induced colitis (Figures 1B–1D and S1). Groups of streptomycin-treated

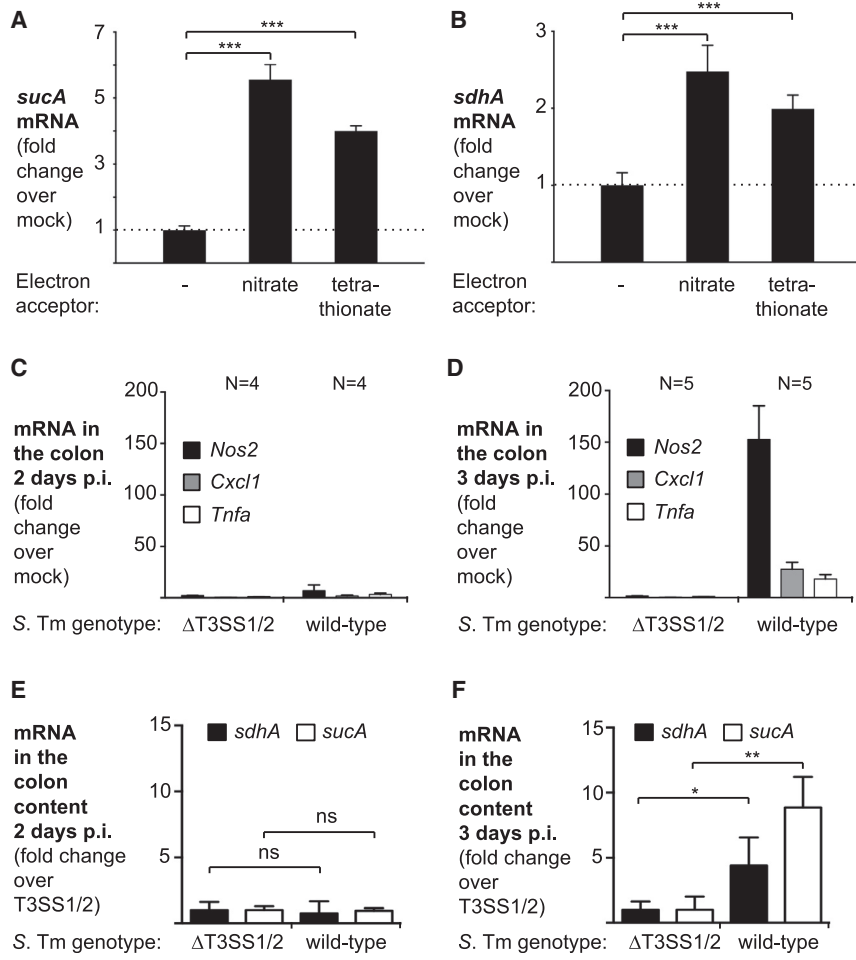


Figure 2. Effect of Gut Inflammation and Electron Acceptors on *sucA* and *sdhA* Transcription

(A and B) Relative transcription of *sucA* (A) and *sdhA* (B) in mucin broth supplemented with the indicated electron acceptors was determined by qRT-PCR. Transcription of target genes was normalized to 16S rRNA.

(C and D) Streptomycin-pretreated C57BL/6 mice were intragastrically inoculated with the *S. Typhimurium* wild-type strain, an *ΔinvA ΔspiB* (Δ T3SS1/2) mutant, or mock treated (LB broth). mRNA levels of *Nos2* (black bars), *Cxcl1* (gray bars), and *Tnfa* (white bars) in the colonic tissue was determined by qRT-PCR 2 days (C) and 3 days (D) post infection (p.i.).

Transcription was normalized to *Gapdh* mRNA. (E and F) Bacterial RNA was extracted from the colon content. Relative transcription of *sdhA* (black bars) and *sucA* (white bars) normalized to *S. Typhimurium* 16S rRNA was determined by qRT-PCR 2 days (E) and 3 days (F) after infection.

Bars represent geometric means, error bars represent the SE. * $p < 0.05$, ** $p < 0.01$, *** $p < 0.001$; ns, not statistically significant. The number of animals per group (N) is indicated above each bar. See also Figure S2.

responses. These experiments raised the possibility that *S. Typhimurium* uses a complete TCA cycle during infection.

Exogenous Electron Acceptors Affect the *S. Typhimurium* TCA Cycle *In Vitro* and *In Vivo*

Addition of the alternative electron acceptor nitrate to anaerobic culture me-

C57BL/6 mice (Barthel et al., 2003) were intragastrically inoculated with an equal mixture of the *S. Typhimurium* wild-type strain (AJB715) and an *ΔsdhA* mutant, or mock treated. Four days after infection, the bacterial load for each strain was determined in the colonic and cecal content by plating on selective media and the ratio of wild-type bacteria to mutant bacteria (competitive index) calculated (Figures 1C and 1D). Interestingly, the *S. Typhimurium* wild-type strain was recovered in higher numbers than the *ΔsdhA* mutant, suggesting that Sdh activity was required for efficient colonization of the gut during infection.

Since the TCA cycle is an essential component for the intermediary metabolism, we were concerned that TCA-cycle mutants were generally impaired for growth. We therefore sought to determine the fitness of TCA-cycle mutants in the absence of inflammation. *S. Typhimurium* employs two type 3 secretion systems to invade non-phagocytic epithelial cells and to mediate replication in the mucosa, respectively (Galan and Curtiss, 1989; Hensel et al., 1998). Mutants lacking both type 3 secretion systems (T3SS1/2; *ΔinvA ΔspiB*) do not induce overt inflammatory responses (Figures 1B and S1A–S1C) and colonize the gut lumen to a limited extent (Coombes et al., 2005; Hapfelmeier et al., 2004, 2005). The T3SS1/2 and T3SS1/2 *ΔsdhA* mutants were recovered in similar numbers (Figures 1C and 1D), indicating that Sdh activity is dispensable in the absence of inflammatory

media can induce expression of TCA-cycle enzymes in *Escherichia coli* K-12; however, this phenomenon only occurs in the absence of the regulatory protein ArcA (Perrenoud and Sauer, 2005; Prohl et al., 1998; Wimpenny and Cole, 1967). During mucosal inflammation, alternative electron acceptors such as nitrate and tetrathionate occur as by-products of the oxidative burst (Winter et al., 2010). To test whether alternative electron acceptors could influence the TCA cycle in *S. Typhimurium*, we cultured mixtures of the *S. Typhimurium* wild-type strain and isogenic mutants deficient in TCA-cycle enzymes in mucin broth under anaerobic conditions for 16 hr. The wild-type strain outcompeted the *ΔsucAB*, *ΔsucCD*, and *ΔsdhA* mutant when nitrate or tetrathionate was added to the growth media while no growth advantage was apparent in the absence of exogenous electron acceptors (Figures 1E–1G). This outcome indicated that alternative electron acceptors are sufficient to alter operation of the TCA cycle in *S. Typhimurium*.

Next, we investigated whether nitrate and tetrathionate increase transcription of *sucA* and *sdhA* during anaerobic growth in mucin broth. RNA was extracted after 16 hr and *sucA* and *sdhA* mRNA levels were determined by qRT-PCR (Figures 2A and 2B). Transcription of *sucA* and *sdhA* increased significantly in the presence of alternative electron acceptors. We then determined the transcriptome of *S. Typhimurium* during colonization of the intestinal tract (Figure S2). To this end, we colonized gnotobiotic

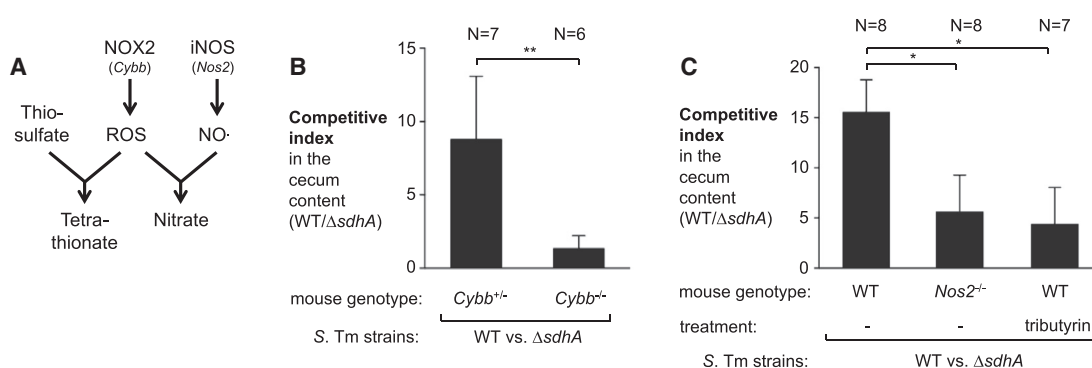


Figure 3. Impact of Inflammation-Derived Electron Acceptors on the TCA Cycle during Infection

(A) Simplified schematic outlining the contribution of NADPH oxidase 2 (NOX2) and inducible nitric oxide synthase (iNOS) to the generation of tetrathionate and nitrate via reactive oxygen species (ROS) and nitric oxide (NO).

(B) Streptomycin-pretreated female $Cybb^{+/-}$ and $Cybb^{-/-}$ mice on the C57BL/6 background were intragastrically inoculated with the S. Tm wild-type strain and a $\Delta sdhA$ mutant. The competitive index in the cecal content was determined after 4 days.

(C) Streptomycin-pretreated C57BL/6 wild-type mice and $Nos2$ -deficient mice were inoculated with a mixture of the S. Tm wild-type strain and a $\Delta sdhA$ mutant. One group was treated with tributyrin as indicated. The competitive index in the cecal content was determined 4 days post infection.

Bars represent geometric means, error bars represent the SE. *p < 0.05, **p < 0.01. The number of animals per group (N) is indicated above each bar.

mice with the S. Tm wild-type strain and performed RNA sequencing (RNA-seq) on RNA extracted from cecal content. A comparison with a published transcriptome database of S. Tm cultured in various *in vitro* conditions (Kroger et al., 2013) showed that the *in vivo* transcriptome formed a state distinct from all *in vitro* conditions in the database (Figure S2A). To assess the overall metabolic state, we compared normalized mRNA levels of selected metabolic enzymes under aerobic and anaerobic culture conditions *in vitro* and in the mouse model (Figures S2B–S2G). Transcription of general housekeeping enzymes such as glyceraldehyde-3-phosphate dehydrogenase (*gapA*), acetate kinase (*ackA*), and phosphate acetyltransferase (*pta*) was comparable in all three conditions (Figure S2B). Consistent with the notion that nitrate and tetrathionate are inducers of the respective reductase operons (Hensel et al., 1999; Rabin and Stewart, 1993), transcription of the tetrathionate reductase, nitrate reductase-1, and the periplasmic nitrate reductase in the murine cecum was increased compared with standard aerobic and anaerobic *in vitro* conditions (Figures S2C–S2E). Furthermore, transcription of *sucAB*, *sucCD*, and *sdh* in the murine model was found to be most similar to growth under aerobic *in vitro* conditions (Figure S2F), which was suggestive of an overall oxidative central metabolism in S. Tm during gut colonization.

We then explored whether inflammation alters expression of key TCA-cycle enzymes in the streptomycin-treated mouse model (Figures 2C–2F). A marked increase in pro-inflammatory markers was observed 3 days after infection (Figures 2D and S1C). Low levels of inflammation were noted early during infection with the wild-type strain (2 days after infection; Figure 2C) and when mice were infected with a T3SS1/2-deficient mutant (Figures 2C and 2D). Transcription of *sdhA* and *sucA* in the S. Tm wild-type strain and the T3SS1/2-deficient mutant were similar 2 days after infection (Figure 2E). Concomitant with the onset of inflammation 3 days after infection, the wild-type strain exhibited a significant increase in *sdhA* and *sucA* mRNA levels compared with the $\Delta T3SS1/2$ mutant (Figure 2F), indicating

that increased levels of mucosal inflammation correlate with increased expression of S. Tm TCA-cycle enzymes.

During *Salmonella* infection, neutrophils infiltrating the mucosa undergo an oxidative burst with the release of reactive oxygen species (ROS) and reactive nitrogen species (RNS) (Figure 3A). NADPH oxidase 2 (NOX2, PHOX), comprising the two chains CYBA and CYBB, catalyzes the first step in the generation of ROS. Inducible nitric oxide synthase (iNOS) is the sole source of nitric oxide. Oxidation of thiosulfate by ROS yields tetrathionate in the gut lumen (Winter et al., 2010) while peroxide can react with nitric oxide to form peroxynitrite, an RNS that decomposes to nitrate (Winter et al., 2013). To assess whether availability of tetrathionate and nitrate affects the S. Tm TCA cycle during infection, we repeated the competitive colonization assay in NOX2 ($Cybb$)- and iNOS ($Nos2$)-deficient mice. In heterozygous $Cybb^{+/-}$ littermate controls, the S. Tm wild-type strain outcompeted the $sdhA$ mutant, while this competitive fitness advantage was abrogated in homozygous $Cybb$ -deficient animals (Figure 3B). The fitness advantage conferred by Sdh activity was significantly reduced in $Nos2$ -deficient mice but not completely abrogated as in the $Cybb$ -deficient mice, suggesting that both tetrathionate and nitrate likely contribute to changes in the central metabolism of S. Tm *in vivo* (Figure 3C). During S. Tm infection, butyrate-producing *Clostridia* spp. are diminished from the gut microbiota (Rivera-Chavez et al., 2016). Depletion of butyric acid, the main carbon source of intestinal epithelial cells, causes a perturbation in the epithelial metabolism, and small amounts of oxygen become available at the mucosal interface. Thus we considered the possibility that, in addition to nitrate and tetrathionate, molecular oxygen could influence the direction of the TCA cycle in the mammalian gut lumen. Supplementation with tributyrin, a source of butyrate that prevents oxygen leakage into the gut lumen (Rivera-Chavez et al., 2016), moderately reduced the competitive fitness of the wild-type strain over the $sdhA$ mutant (Figure 3C). Collectively, these data suggest that availability of exogenous electron acceptors, such as

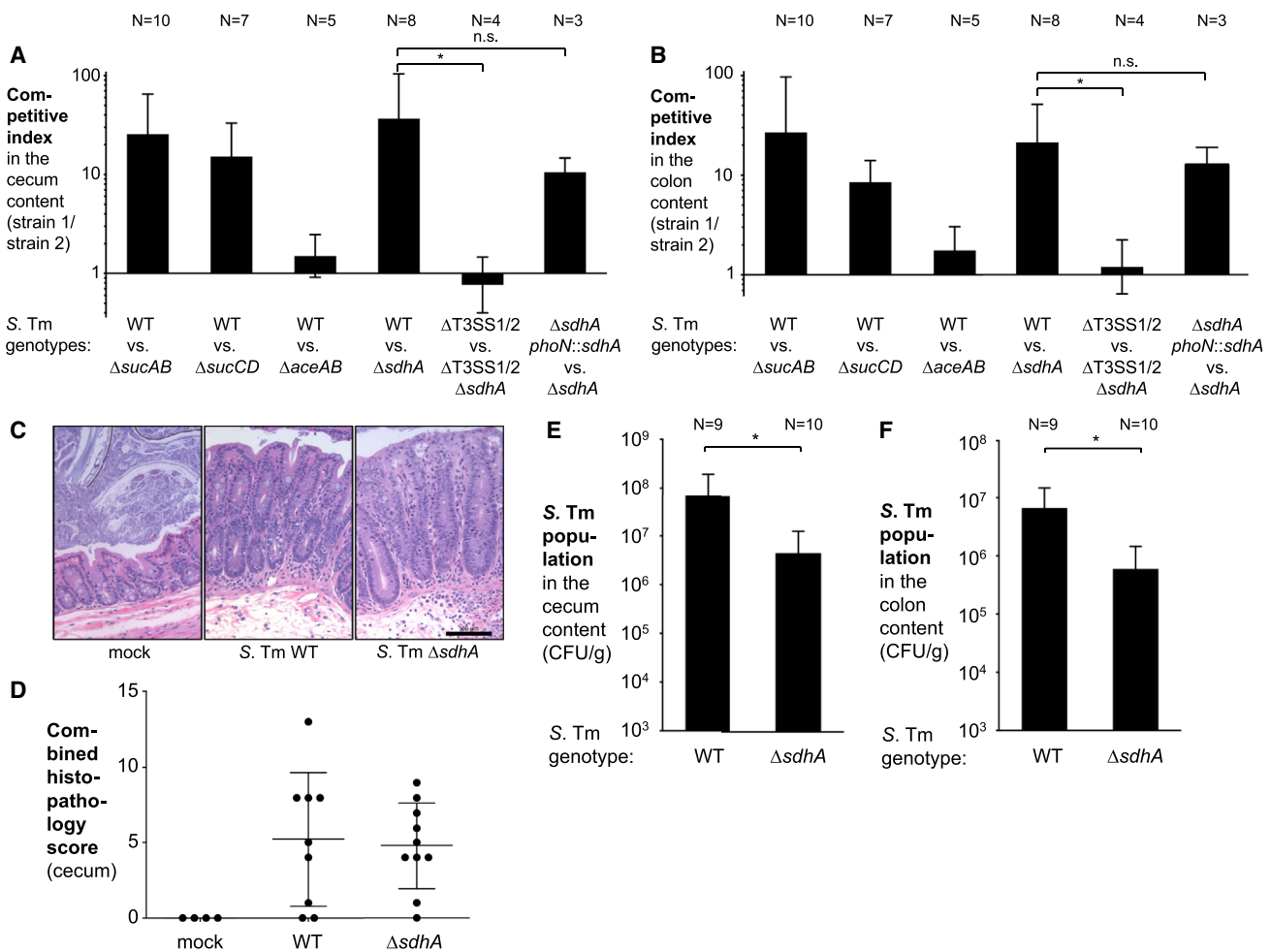


Figure 4. Sdh, α -Ketoglutarate Dehydrogenase, and Succinyl-CoA Synthetase Activity Contribute to Fitness of S. Tm in Mice with Native Microbiota

(A and B) CBA mice were infected with an equal mixture of the indicated S. Tm strains by the intragastric route. Competitive index of the indicated strains in the cecal (A) and colonic lumen (B) 7 days after infection. WT, S. Tm wild-type strain; Δ T3SS1/2, Δ invA Δ spiB mutant. Bars represent geometric means, error bars represent the SE. *p < 0.05; ns, not statistically significant.

(C–F) CBA mice were intragastrically infected with the S. Tm wild-type strain or a Δ sdhA mutant. (C) Representative images of H&E-stained cecal tissue. Scale bar, 100 μ m. (D) Combined histopathology score of pathological lesions in the cecum. Each dot represents one animal. The lines represent the mean \pm SE. (E and F) S. Tm population levels in the cecum (E) and colon (F) content 7 days after infection. Bars represent geometric means, error bars represent the SE. *p < 0.05. The number of animals per group (N) is indicated above each bar. See also Figure S3.

nitrate, tetrathionate, and oxygen, alter the central metabolism of S. Tm in a mouse model of infection.

A Complete TCA Cycle Enhances S. Tm Fitness in Competition with the Native Microbiota

To determine whether a complete TCA cycle might enhance fitness of S. Tm in competition with the unperturbed native gut microbiota, we used CBA mice, which develop neutrophilic inflammation of the large intestine after 7–10 days (Figures S3A and S3B). The competitive fitness of the S. Tm wild-type strain and mutants lacking TCA-cycle enzymes was determined 7 days after infection (Figures 4A and 4B). The S. Tm wild-type strain outcompeted the Δ sucAB, Δ sucCD, and Δ sdhA mutants. The glyoxylate shunt, a pathway bypassing α -ketoglutarate dehydrogenase and succinyl-CoA synthetase, was dispensable

for growth in the inflamed gut since a Δ aceAB mutant did not exhibit a fitness defect under the conditions tested (Figures 4A and 4B). Sdh activity did not confer a fitness advantage in the absence of inflammation (Δ invA Δ spiB mutant background) in the CBA mouse model. Complementation of the $sdhA$ mutant by introducing the $sdhA$ promoter and coding sequence into the neutral *phoN* recapitulated the phenotype of the wild-type strain (Figures 4A and 4B). Similar observations were made using another S. Tm isolate, SL1344 (Figure S3C).

To determine whether a complete TCA cycle contributed to growth of S. Tm in direct competition with the native microbiota, we infected groups of CBA animals intragastrically with either the S. Tm wild-type strain or the Δ sdhA mutant (single infection). Both strains induced host inflammation to a similar degree (Figures 4C, 4D, and S3). However, the $sdhA$ -deficient mutant was

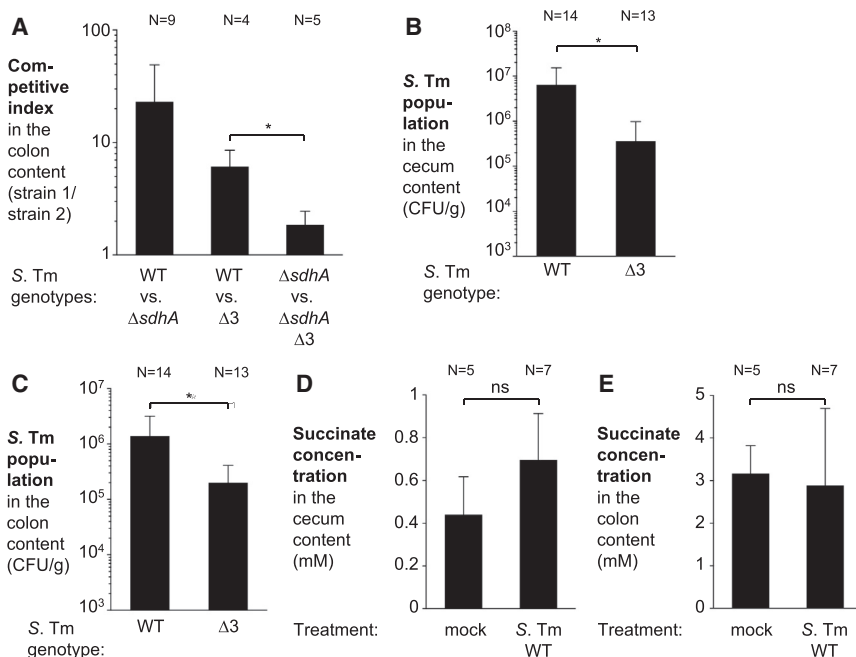


Figure 5. Succinate Uptake and Utilization Confer a Fitness Advantage in Competition with the Native Gut Microbiota

(A) Groups of CBA mice were intragastrically infected with a mixture of the indicated *S. Tm* strains. Seven days after infection, the competitive index in the colon content was determined. Δ3, $\Delta dcuA \Delta dcuB \Delta dctA$ mutant.

(B–E) As indicated, CBA mice were infected with the *S. Tm* wild-type strain (WT), the Δ3 mutant ($\Delta dcuA \Delta dcuB \Delta dctA$ mutant), or mock treated. (B and C) *S. Tm* populations in the cecum (B) and colon content (C) 7 days after infection. (D and E) Succinate concentration in the cecum content (D) and colon content (E) as determined by gas chromatography-tandem mass spectrometry. Bars represent geometric means, error bars represent the SE. * $p < 0.05$; ns, not statistically significant. The number of animals per group (N) is indicated above each bar.

3 mM in the colon content (Figures 5D and 5E). No changes in extracellular succinate levels upon *S. Tm* infection were noted.

recovered at significantly lower numbers than the wild-type strain in the cecum and colon content (29-fold and 80-fold, respectively) 7 days after infection (Figures 4E and 4F). Collectively, the experiments support the idea that switching from a branched to a full TCA cycle is a critical metabolic adaption for *S. Tm* to compete with the native microbiota for colonization of the intestinal tract.

Utilization of Dicarboxylic Acids by *S. Tm*

One potential consequence of the inflammation-associated oxidative central metabolism of *S. Tm* could be that poorly fermentable dicarboxylic acids, such as succinate, could serve as carbon sources by feeding directly into the TCA cycle. To test whether uptake of di- and tricarboxylic acids contributes to growth of *S. Tm* during colitis, we constructed mutants lacking the C4-dicarboxylate carriers DctA (succinate-proton symporter), DcuA (succinate-proton symporter), and DcuB (fumarate-succinate antiporter) ($\Delta dcuA \Delta dcuB \Delta dctA$ mutant; Δ3 mutant). In CBA mice, the *S. Tm* wild-type strain outcompeted the Δ3 mutant by 5-fold (Figure 5A). Similarly, the Δ3 mutant exhibited a gut colonization defect compared with the wild-type strain in single infection experiments (Figures 5B and 5C), indicating that C4-dicarboxylate uptake enhances fitness of *S. Tm* in the lumen of the mammalian intestine.

Microbiota-Derived Succinate Supports Growth of *S. Tm* during Infection

Obligate anaerobic commensals, in particular *Bacteroides* spp., use a branched TCA cycle to support fumarate respiration. The end product of fumarate reduction, succinate, is secreted into the extracellular environment. In the human gut, luminal succinate levels range from approximately 0.5 to 5 mM (Cummings et al., 1987; Meijer-Severs and van Santen, 1987; Rubinstein et al., 1969). In the CBA mouse model, the concentration of succinate was found to be about 0.4 mM in the cecum content and

Based on these findings, we hypothesized that *Bacteroides*-derived succinate could be utilized by *S. Tm* as a consequence of a complete TCA cycle. To investigate this idea, we cultured *B. thetaiotaomicron* in mucin broth for 3 days. Growth of *B. thetaiotaomicron* led to the accumulation of succinate in the filter-sterilized culture supernatant (Figure 6A). Next, we determined anaerobic growth of *S. Tm* using the *B. thetaiotaomicron*-fermented mucin as a growth medium. In the absence of any exogenous electron acceptor, C4-dicarboxylate transporters did not provide a growth advantage. However, when nitrate was added to the medium to switch from a branched to a complete TCA cycle, the wild-type strain outcompeted the $\Delta dcuA \Delta dcuB \Delta dctA$ mutant (Figure 6B).

C4-dicarboxylate transporters can facilitate the uptake of succinate and several other dicarboxylates, such as fumarate, aspartate, malate, and tartrate (reviewed in Unden and Kleefeld, 2004). In the absence of Sdh activity ($\Delta sdhA$ versus $\Delta sdhA$ Δ3 mutant), the growth advantage conferred by C4-dicarboxylate transporters was abolished, supporting the notion that the growth advantage conferred by these uptake systems was indeed due to succinate uptake (Figure 6B). Collectively, these experiments demonstrate that *B. thetaiotaomicron*-derived succinate can be utilized by *S. Tm* in the presence of exogenous electron acceptors *in vitro*.

Next, we investigated succinate uptake and utilization in gnotobiotic mice (genetically resistant Swiss Webster mice) and mice that had been mono-associated with *B. thetaiotaomicron*. Infection with *S. Tm* induced significant pathological changes in the cecal and colonic mucosa in both groups (Figures 6C, S4, S5A, and S5B). Consistent with the idea that succinate is derived from the gut microbiota, C4-dicarboxylate uptake (Δ3 mutant) and Sdh activity ($\Delta sdhA$ mutant) were dispensable for intestinal colonization during infection of gnotobiotic mice (Figures 6D, 6E, and S5C). Importantly, mono-colonization with *B. thetaiotaomicron* was sufficient to reinstate the fitness advantage conferred by

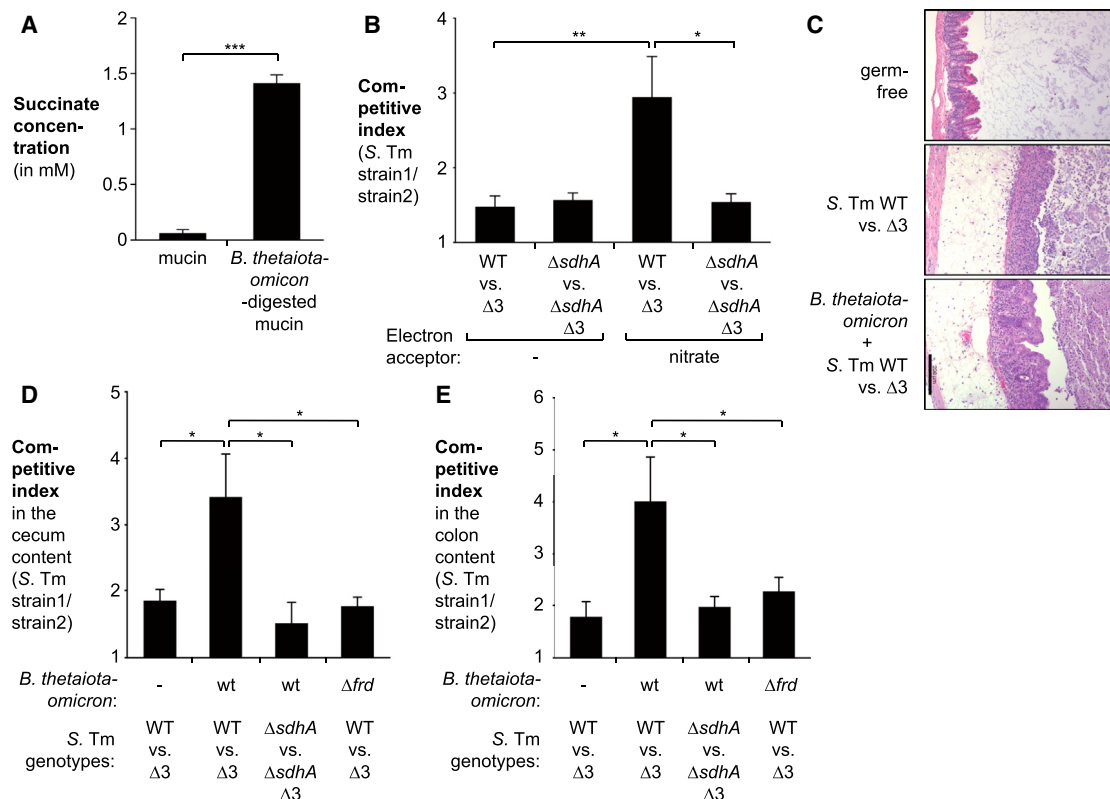


Figure 6. Microbiota-Derived Succinate Enhances *S. Tm* Growth during Infection

(A and B) Mucin broth was inoculated with *B. thetaiotaomicron* and incubated anaerobically for 3 days. (A) Concentration of succinate in the supernatant. (B) The filter-sterilized *B. thetaiotaomicron*-digested mucin broth was inoculated with the indicated *S. Tm* strains and the competitive index after 16 hr of anaerobic growth determined. Sodium nitrate (40 mM) was added as indicated.

(C–E) Germ-free Swiss Webster mice and mice mono-associated with the *B. thetaiotaomicron* wild-type strain (wt) or a *ΔfrdCAB* (*Δfrd*) mutant were infected with an equal mixture of the *S. Tm* wild-type strain (WT) and the *ΔdcuA ΔdcuB ΔdctA* (*Δ3*) mutant or a mixture of an *S. Tm* *ΔsdhA* and a *ΔsdhA ΔdcuA ΔdcuB ΔdctA* (*ΔsdhA Δ3*) mutant. Samples were analyzed 3 days after infection. (C) Representative images of H&E-stained sections of the cecum. Scale bar, 200 μm. (D and E) Competitive index in the cecum (D) and colon content (E).

Bars represent geometric means, error bars represent the SE. *p < 0.05; **p < 0.01; ***p < 0.001. The number of animals per group (N) is indicated above each bar. See also Figures S4–S6.

C4-dicarboxylate uptake (Figures 6D, 6E, and S5C). In the absence of succinate degradation (*ΔsdhA* versus *ΔsdhA Δ3*), the effect of C4-dicarboxylate uptake on competitive fitness was minimal in the gnotobiotic mouse model as well as in conventionally raised CBA mice (Figures 5A, 6D, and 6E). We also generated a *B. thetaiotaomicron* that is unable to generate succinate *in vitro* and *in vivo* (Figures S6A and S6B) due to a lack of fumarate reductase activity (*Δfrd*). In contrast to the *B. thetaiotaomicron* wild-type strain, mono-association with the *B. thetaiotaomicron* *Δfrd* mutant was unable to restore the fitness advantage C4-dicarboxylate uptake in *S. Tm* (Figures 6D and 6E). Metabolic profiling of large intestinal contents of mice mono-associated with the *B. thetaiotaomicron* wild-type strain and the isogenic *Δfrd* mutant revealed an absence of succinate in *Δfrd* colonized mice (Figures S6B and S6C) and a compensatory increase in lactate levels (Figure S6C). Lactate is not known to be transported by C4-dicarboxylate carriers and does not serve as a substrate for Sdh. Collectively, these experiments demonstrate that microbiota-derived succinate is taken up and utilized by *S. Tm* during colonization of the inflamed intestinal tract.

DISCUSSION

The central metabolism of *S. Tm* has been analyzed extensively *in vitro* and in murine models of systemic infection. *S. Tm* mutants lacking key TCA-cycle enzymes are defective for replication in tissue at systemic sites (Mercado-Lubo et al., 2008, 2009; Tchawa Yimga et al., 2006). TCA-cycle reactions are predicted to have high metabolic conversion rates during growth in the spleen (Steeb et al., 2013). Furthermore, the central metabolism of *S. Tm* shapes host-microbe interactions during infection of macrophages. A complete oxidative TCA cycle is of critical importance for *S. Tm* to avoid pyroptotic cell death in macrophages in cell culture (Wynosky-Dolfi et al., 2014). Activated macrophages restrict bacterial metabolism by releasing RNS to deactivate the lipoamide-dependent enzymes pyruvate and α-ketoglutarate dehydrogenase (Richardson et al., 2011). Infection of immune-competent individuals with non-typhoidal *Salmonella* serotypes results in a self-limiting gastroenteritis, and no bacterial dissemination is observed. Curiously, the central metabolism of *S. Tm* during

natural infection, i.e., during *Salmonella*-induced colitis, has not been investigated.

Strict anaerobic commensals have evolved to successfully compete for carbon and energy sources in the nutrient-limiting environment of the healthy large intestine. As a combined function of the metabolism of the bacterial community, all energetically valuable compounds are depleted, hampering intrusion of the ecosystem by enteric pathogens. To overcome this colonization resistance, *S. Tm* triggers an acute mucosal inflammatory response, which creates a niche in the lumen of the intestine that is suitable for the outgrowth of *S. Tm* over other commensals (Barman et al., 2008; Stecher et al., 2007). One prominent change in the gut environment during *S. Tm* infection is the production of oxidized compounds such as nitrate and tetrathionate as by-products of the oxidative burst by infiltrating neutrophils (Lopez et al., 2012; Winter et al., 2010). Unlike obligate anaerobic commensals, *S. Tm* utilizes these oxidized compounds as electron acceptors for the electron transport chain. Here we show that mucosal inflammation significantly alters the central metabolism of the *S. Tm* population residing in the gut lumen. Alternative electron acceptors, such as nitrate, change the direction of the TCA from a branched set of reactions to a full, oxidative TCA cycle in the mammalian intestine.

An oxidative central metabolism could enhance growth of *S. Tm* through several mechanisms. Carbon sources that are fully or partially degraded to acetyl-CoA could enter the TCA cycle and be oxidized to CO₂ *in vivo*. *In vitro*, *Salmonella* is known to utilize a great variety of compounds as the sole carbon source during aerobic conditions (Gutnick et al., 1969). In the murine gut, only few carbon sources have been identified, such as ethanamine, 1,2-propanediol, and fructose-asparagine (Ali et al., 2014; Faber et al., 2017; Thienennimitr et al., 2011). An oxidative TCA cycle may explain why utilization of these compounds *in vivo* strictly requires respiration. In this study, we demonstrate that C4-dicarboxylic acids may serve as nutrients for *S. Tm* during infection. Specifically, uptake and utilization of succinate enhances *S. Tm* growth in the inflamed gut. Succinate is generated as a predominant fermentation end product of *Bacteroides* in the reductive branch of a split TCA cycle. During inflammation, this metabolism is mirrored by *S. Tm* as the set of reactions that make up the reductive branch is reversed. This metabolic adaptation to the inflamed gut allows the pathogen to utilize a microbiota-derived metabolic waste product as a nutrient.

Since the phenotype of the C4-dicarboxylate uptake mutant only partially recapitulated the phenotype of the *sdhA* mutant, it is likely that the oxidative TCA cycle enhances *S. Tm* fitness by additional mechanisms. For example, in *Proteus mirabilis*, an oxidative TCA cycle is required to generate energy for swarming (Alteri et al., 2012). Flagella-mediated motility is required for *S. Tm* to efficiently colonize the inflamed gut lumen (Stecher et al., 2008). Furthermore, it is possible that other carbon sources could enter the oxidative TCA cycle, either as acetyl-CoA or through anaplerotic reactions. Of note, the phenotype of the C4-dicarboxylate uptake mutant was not entirely abolished during infection in gnotobiotic mice, suggesting that dietary or host-derived C4-dicarboxylates might be utilized by *S. Tm* as well. Collectively, an oxidative TCA cycle might give *S. Tm* flexibility in nutrient acquisition and energy generation during colonization of the gastrointestinal tract.

Apart from serving as a nutrient, succinate acts as a cue for some enteric pathogens. Expression of the locus of enterocyte effacement, a major virulence factor of enterohemorrhagic *E. coli*, is regulated *in vivo* by succinate (Curtis et al., 2014). Furthermore, oral antibiotic therapy is associated with blooms of *C. difficile*. In mouse models, an antibiotic-induced perturbation of the microbiota increases the local availability of succinate, which in return supports the expansion of *C. difficile* (Ferreira et al., 2014). Our work shows that microbiota-derived succinate fuels *S. Tm* growth during natural infection without the need for antibiotic treatment, thus identifying a critical microbiota-pathogen interaction in the context of infection of the mammalian host.

STAR★METHODS

Detailed methods are provided in the online version of this paper and include the following:

- KEY RESOURCES TABLE
- CONTACT FOR REAGENT AND RESOURCE SHARING
- EXPERIMENTAL MODEL AND SUBJECT DETAILS
 - Mice
 - Bacterial Culture
- METHOD DETAILS
 - Construction of Plasmids
 - Generation of *S. Tm* Mutants
 - Construction of a *B. thetaiotaomicron* *frd* Mutant
 - Growth of *B. thetaiotaomicron* in Mucin Broth
 - Succinate Concentration Measurement in Digeested Mucin
 - Anaerobic Growth of *S. Tm* in Mucin Broth
 - Animal Models of *S. Tm*-Induced Colitis
 - Quantification of Inflammatory Markers by qRT-PCR
 - Bacterial Gene Expression
 - Histopathology
 - iNOS Expression in Intestinal Tissue by Western Blot
 - Metabolite Profiling and Quantification of Succinate
 - Transcriptional Profile of *S. Tm* in the Large Intestine
- QUANTIFICATION AND STATISTICAL ANALYSIS
 - Statistical Analysis
- DATA AND SOFTWARE AVAILABILITY

SUPPLEMENTAL INFORMATION

Supplemental Information includes six figures and two tables and can be found with this article online at <http://dx.doi.org/10.1016/j.chom.2017.07.018>.

AUTHOR CONTRIBUTIONS

S.E.W., L.V.H., D.C., H.L.A.-P., D.P.B., and R.L.S. designed and conceived the study; L.S., M.G.W., W.Z., E.R.H., C.C.G., C.L.B., and S.E.W. performed all experiments. R.L.S. and T.F.d.C. performed the histopathology analysis. W.Z., D.P.B., and J.K. generated and analyzed the RNA-seq data. All authors contributed to data analysis and writing the manuscript.

ACKNOWLEDGMENTS

Work in the S.E.W. laboratory was funded by the NIH (AI118807, AI103248, AI128151) and the Welch Foundation (I-1858). Work in the L.V.H. laboratory was funded by the NIH (DK070855), the Welch Foundation (I-1874), and the

Howard Hughes Medical Institute. J.K. is supported by the Cancer Prevention and Research Institute of Texas (grant RP150596). The funders had no role in study design, data collection and interpretation, or the decision to submit the work for publication. Any opinions, findings, and conclusions or recommendations expressed in this material are those of the author(s) and do not necessarily reflect the views of the funding agencies. We would like to thank Drs. David Hendrixson, Julie Pfeiffer, and Vanessa Sperandio for helpful discussion, and Madeline Smoot for technical assistance.

Received: July 15, 2016

Revised: June 23, 2017

Accepted: July 28, 2017

Published: August 24, 2017

SUPPORTING CITATIONS

The following references appear in the Supplemental Information: Godinez et al. (2008); Overbergh et al. (2003); Wilson et al. (2008).

REFERENCES

- Ali, M.M., Newsom, D.L., Gonzalez, J.F., Sabag-Daigle, A., Stahl, C., Steidley, B., Dubena, J., Dyszel, J.L., Smith, J.N., Dieye, Y., et al. (2014). Fructose-asparagine is a primary nutrient during growth of *Salmonella* in the inflamed intestine. *PLoS Pathog.* 10, e1004209.
- Alteri, C.J., Himpel, S.D., Engstrom, M.D., and Mobley, H.L. (2012). Anaerobic respiration using a complete oxidative TCA cycle drives multicellular swarming in *Proteus mirabilis*. *MBio* 3, e00365–12.
- Amarasingham, C.R., and Davis, B.D. (1965). Regulation of alpha-ketoglutarate dehydrogenase formation in *Escherichia coli*. *J. Biol. Chem.* 240, 3664–3668.
- Barman, M., Unold, D., Shifley, K., Amir, E., Hung, K., Bos, N., and Salzman, N. (2008). Enteric salmonellosis disrupts the microbial ecology of the murine gastrointestinal tract. *Infect. Immun.* 76, 907–915.
- Barthel, M., Hapfelmeier, S., Quintanilla-Martinez, L., Kremer, M., Rohde, M., Hogardt, M., Pfeffer, K., Russmann, H., and Hardt, W.D. (2003). Pretreatment of mice with streptomycin provides a *Salmonella enterica* serovar *Typhimurium* colitis model that allows analysis of both pathogen and host. *Infect. Immun.* 71, 2839–2858.
- Caporaso, J.G., Kuczynski, J., Stombaugh, J., Bittinger, K., Bushman, F.D., Costello, E.K., Fierer, N., Pena, A.G., Goodrich, J.K., Gordon, J.I., et al. (2010). QIIME allows analysis of high-throughput community sequencing data. *Nat. Methods* 7, 335–336.
- Coombes, B.K., Coburn, B.A., Potter, A.A., Gomis, S., Mirakhur, K., Li, Y., and Finlay, B.B. (2005). Analysis of the contribution of *Salmonella* pathogenicity islands 1 and 2 to enteric disease progression using a novel bovine ileal loop model and a murine model of infectious enterocolitis. *Infect. Immun.* 73, 7161–7169.
- Crawford, R.W., Keestra, A.M., Winter, S.E., Xavier, M.N., Tsolis, R.M., Tolstikov, V., and Baumler, A.J. (2012). Very long O-antigen chains enhance fitness during *Salmonella*-induced colitis by increasing bile resistance. *PLoS Pathog.* 8, e1002918.
- Cronan, J.E., and Laporte, D. (2013). Tricarboxylic acid cycle and glyoxylate bypass. *EcoSal Plus*. <http://dx.doi.org/10.1128/ecosalplus.3.5.2>.
- Crost, E.H., Tailford, L.E., Le Gall, G., Fons, M., Henrissat, B., and Juge, N. (2013). Utilisation of mucin glycans by the human gut symbiont *Ruminococcus gnavus* is strain-dependent. *PLoS One* 8, e76341.
- Cummings, J.H., Pomare, E.W., Branch, W.J., Naylor, C.P., and Macfarlane, G.T. (1987). Short chain fatty acids in human large intestine, portal, hepatic and venous blood. *Gut* 28, 1221–1227.
- Curtis, M.M., Hu, Z., Klimko, C., Narayanan, S., Deberardinis, R., and Sperandio, V. (2014). The gut commensal *Bacteroides thetaiotaomicron* exacerbates enteric infection through modification of the metabolic landscape. *Cell Host Microbe* 16, 759–769.
- Cuskin, F., Lowe, E.C., Temple, M.J., Zhu, Y., Cameron, E.A., Pudlo, N.A., Porter, N.T., Urs, K., Thompson, A.J., Cartmell, A., et al. (2015). Human gut Bacteroidetes can utilize yeast mannan through a selfish mechanism. *Nature* 517, 165–169.
- Elam, O., Zarecki, R., Oberhardt, M., Ursell, L.K., Kupiec, M., Knight, R., Gophna, U., and Rupp, E. (2014). Glycan degradation (GlyDeR) analysis predicts mammalian gut microbiota abundance and host diet-specific adaptations. *MBio* 5, e01526–14.
- El Kaoutari, A., Armougou, F., Gordon, J.I., Raoult, D., and Henrissat, B. (2013). The abundance and variety of carbohydrate-active enzymes in the human gut microbiota. *Nat. Rev. Microbiol.* 11, 497–504.
- Faber, F., Thiennimitr, P., Spiga, L., Byndloss, M.X., Litvak, Y., Lawhon, S., Andrews-Polymenis, H.L., Winter, S.E., and Baumler, A.J. (2017). Respiration of microbiota-derived 1,2-propanediol drives salmonella expansion during colitis. *PLoS Pathog.* 13, e1006129.
- Ferreira, J.A., Wu, K.J., Hryckowian, A.J., Bouley, D.M., Weimer, B.C., and Sonnenburg, J.L. (2014). Gut microbiota-produced succinate promotes *C. difficile* infection after antibiotic treatment or motility disturbance. *Cell Host Microbe* 16, 770–777.
- Fischbach, M.A., and Sonnenburg, J.L. (2011). Eating for two: how metabolism establishes interspecies interactions in the gut. *Cell Host Microbe* 10, 336–347.
- Flint, H.J., Scott, K.P., Duncan, S.H., Louis, P., and Forano, E. (2012). Microbial degradation of complex carbohydrates in the gut. *Gut Microbes* 3, 289–306.
- Galan, J.E., and Curtiss, R., 3rd (1989). Cloning and molecular characterization of genes whose products allow *Salmonella typhimurium* to penetrate tissue culture cells. *Proc. Natl. Acad. Sci. USA* 86, 6383–6387.
- Godinez, I., Haneda, T., Raffatelli, M., George, M.D., Paixao, T.A., Rolan, H.G., Santos, R.L., Dandekar, S., Tsolis, R.M., and Baumler, A.J. (2008). T cells help to amplify inflammatory responses induced by *Salmonella enterica* serotype *Typhimurium* in the intestinal mucosa. *Infect. Immun.* 76, 2008–2017.
- Gunn, J.S. (2008). The *Salmonella* PmrAB regulon: lipopolysaccharide modifications, antimicrobial peptide resistance and more. *Trends Microbiol.* 16, 284–290.
- Gutnick, D., Calvo, J.M., Klopotowski, T., and Ames, B.N. (1969). Compounds which serve as the sole source of carbon or nitrogen for *Salmonella typhimurium* LT-2. *J. Bacteriol.* 100, 215–219.
- Hapfelmeier, S., Ehrbar, K., Stecher, B., Barthel, M., Kremer, M., and Hardt, W.D. (2004). Role of the *Salmonella* pathogenicity island 1 effector proteins SipA, SopB, SopE, and SopE2 in *Salmonella enterica* subspecies 1 serovar *Typhimurium* colitis in streptomycin-pretreated mice. *Infect. Immun.* 72, 795–809.
- Hapfelmeier, S., Stecher, B., Barthel, M., Kremer, M., Muller, A.J., Heikenwalder, M., Stallmach, T., Hensel, M., Pfeffer, K., Akira, S., et al. (2005). The *Salmonella* pathogenicity island (SPI)-2 and SPI-1 type III secretion systems allow *Salmonella* serovar *typhimurium* to trigger colitis via MyD88-dependent and MyD88-independent mechanisms. *J. Immunol.* 174, 1675–1685.
- Hensel, M., Hinsley, A.P., Nikolaus, T., Sawers, G., and Berks, B.C. (1999). The genetic basis of tetrathionate respiration in *Salmonella typhimurium*. *Mol. Microbiol.* 32, 275–287.
- Hensel, M., Shea, J.E., Waterman, S.R., Mundy, R., Nikolaus, T., Banks, G., Vazquez-Torres, A., Gleeson, C., Fang, F.C., and Holden, D.W. (1998). Genes encoding putative effector proteins of the type III secretion system of *Salmonella* pathogenicity island 2 are required for bacterial virulence and proliferation in macrophages. *Mol. Microbiol.* 30, 163–174.
- Hoiseth, S.K., and Stocker, B.A. (1981). Aromatic-dependent *Salmonella typhimurium* are non-virulent and effective as live vaccines. *Nature* 291, 238–239.
- Iuchi, S., and Lin, E.C. (1988). arcA (dye), a global regulatory gene in *Escherichia coli* mediating repression of enzymes in aerobic pathways. *Proc. Natl. Acad. Sci. USA* 85, 1888–1892.
- Kingsley, R.A., Humphries, A.D., Weening, E.H., De Zoete, M.R., Winter, S., Papaconstantinopoulou, A., Dougan, G., and Baumler, A.J. (2003).

- Molecular and phenotypic analysis of the CS54 island of *Salmonella enterica* serotype *typhimurium*: identification of intestinal colonization and persistence determinants. *Infect. Immun.* 71, 629–640.
- Kingsley, R.A., Reissbrodt, R., Rabsch, W., Ketley, J.M., Tsolis, R.M., Everest, P., Dougan, G., Baumler, A.J., Roberts, M., and Williams, P.H. (1999). Ferrioxamine-mediated iron(III) utilization by *Salmonella enterica*. *Appl. Environ. Microbiol.* 65, 1610–1618.
- Koropatkin, N.M., Martens, E.C., Gordon, J.I., and Smith, T.J. (2008). Starch catabolism by a prominent human gut symbiont is directed by the recognition of amylose helices. *Structure* 16, 1105–1115.
- Koropatkin, N.M., Cameron, E.A., and Martens, E.C. (2012). How glycan metabolism shapes the human gut microbiota. *Nat. Rev. Microbiol.* 10, 323–335.
- Kroger, C., Colgan, A., Srikumar, S., Handler, K., Sivasankaran, S.K., Hammarlof, D.L., Canals, R., Grissom, J.E., Conway, T., Hokamp, K., et al. (2013). An infection-relevant transcriptomic compendium for *Salmonella enterica* serovar *typhimurium*. *Cell Host Microbe* 14, 683–695.
- Langmead, B., and Salzberg, S.L. (2012). Fast gapped-read alignment with Bowtie 2. *Nat. Methods* 9, 357–359.
- Lawes, M., and Maloy, S. (1995). MudSaci, a transposon with strong selectable and counterselectable markers: use for rapid mapping of chromosomal mutations in *Salmonella typhimurium*. *J. Bacteriol.* 177, 1383–1387.
- Lawley, T.D., Bouley, D.M., Hoy, Y.E., Gerke, C., Relman, D.A., and Monack, D.M. (2008). Host transmission of *Salmonella enterica* serovar *Typhimurium* is controlled by virulence factors and indigenous intestinal microbiota. *Infect. Immun.* 76, 403–416.
- Liao, Y., Smyth, G.K., and Shi, W. (2014). featureCounts: an efficient general purpose program for assigning sequence reads to genomic features. *Bioinformatics* 30, 923–930.
- Liu, J.Z., Jellbauer, S., Poe, A.J., Ton, V., Pesciaroli, M., Kehl-Fie, T.E., Restrepo, N.A., Hosking, M.P., Edwards, R.A., Battistoni, A., et al. (2012). Zinc sequestration by the neutrophil protein calprotectin enhances *Salmonella* growth in the inflamed gut. *Cell Host Microbe* 11, 227–239.
- Lopez, C.A., Winter, S.E., Rivera-Chavez, F., Xavier, M.N., Poon, V., Nuccio, S.P., Tsolis, R.M., and Baumler, A.J. (2012). Phage-mediated acquisition of a type III secreted effector protein boosts growth of salmonella by nitrate respiration. *MBio* 3, e00143–12.
- Lupp, C., Robertson, M.L., Wickham, M.E., Sekirov, I., Champion, O.L., Gaynor, E.C., and Finlay, B.B. (2007). Host-mediated inflammation disrupts the intestinal microbiota and promotes the overgrowth of Enterobacteriaceae. *Cell Host Microbe* 2, 119–129.
- Macy, J., Probst, I., and Gottschalk, G. (1975). Evidence for cytochrome involvement in fumarate reduction and adenosine 5'-triphosphate synthesis by *Bacteroides fragilis* grown in the presence of hemin. *J. Bacteriol.* 123, 436–442.
- Maier, L., Vyas, R., Cordova, C.D., Lindsay, H., Schmidt, T.S., Brugiroux, S., Periaswamy, B., Bauer, R., Sturm, A., Schreiber, F., et al. (2013). Microbiota-derived hydrogen fuels *Salmonella typhimurium* invasion of the gut ecosystem. *Cell Host Microbe* 14, 641–651.
- Martens, E.C., Kelly, A.G., Tauzin, A.S., and Brumer, H. (2014). The devil lies in the details: how variations in polysaccharide fine-structure impact the physiology and evolution of gut microbes. *J. Mol. Biol.* 426, 3851–3865.
- Meijer-Severs, G.J., and van Santen, E. (1987). Short-chain fatty acids and succinate in feces of healthy human volunteers and their correlation with anaerobe cultural counts. *Scand. J. Gastroenterol.* 22, 672–676.
- Mercado-Lubo, R., Gauger, E.J., Leatham, M.P., Conway, T., and Cohen, P.S. (2008). A *Salmonella enterica* serovar *typhimurium* succinate dehydrogenase/fumarate reductase double mutant is avirulent and immunogenic in BALB/c mice. *Infect. Immun.* 76, 1128–1134.
- Mercado-Lubo, R., Leatham, M.P., Conway, T., and Cohen, P.S. (2009). *Salmonella enterica* serovar *Typhimurium* mutants unable to convert malate to pyruvate and oxaloacetate are avirulent and immunogenic in BALB/c mice. *Infect. Immun.* 77, 1397–1405.
- Miller, V.L., and Mekalanos, J.J. (1988). A novel suicide vector and its use in construction of insertion mutations: osmoregulation of outer membrane proteins and virulence determinants in *Vibrio cholerae* requires toxR. *J. Bacteriol.* 170, 2575–2583.
- Overbergh, L., Giulietti, A., Valckx, D., Decallonne, R., Bouillon, R., and Mathieu, C. (2003). The use of real-time reverse transcriptase PCR for the quantification of cytokine gene expression. *J. Biomol. Tech.* 14, 33–43.
- Pal, D., Venkova-Canova, T., Srivastava, P., and Chatteraj, D.K. (2005). Multipartite regulation of rctB, the replication initiator gene of *Vibrio cholerae* chromosome II. *J. Bacteriol.* 187, 7167–7175.
- Perrenoud, A., and Sauer, U. (2005). Impact of global transcriptional regulation by ArcA, ArcB, Cra, Crp, Cya, Fnr, and Mlc on glucose catabolism in *Escherichia coli*. *J. Bacteriol.* 187, 3171–3179.
- Porwollik, S., Santiviago, C.A., Cheng, P., Long, F., Desai, P., Fredlund, J., Srikumar, S., Silva, C.A., Chu, W., Chen, X., et al. (2014). Defined single-gene and multi-gene deletion mutant collections in *Salmonella enterica* sv *Typhimurium*. *PLoS One* 9, e99820.
- Prohl, C., Wackwitz, B., Vlad, D., and Unden, G. (1998). Functional citric acid cycle in an arcA mutant of *Escherichia coli* during growth with nitrate under anoxic conditions. *Arch. Microbiol.* 170, 1–7.
- Pudlo, N.A., Urs, K., Kumar, S.S., German, J.B., Mills, D.A., and Martens, E.C. (2015). Symbiotic human gut bacteria with variable metabolic priorities for host mucosal glycans. *MBio* 6, e01282–15.
- Rabin, R.S., and Stewart, V. (1993). Dual response regulators (NarL and NarP) interact with dual sensors (NarX and NarQ) to control nitrate- and nitrite-regulated gene expression in *Escherichia coli* K-12. *J. Bacteriol.* 175, 3259–3268.
- Raffatellu, M., George, M.D., Akiyama, Y., Hornsby, M.J., Nuccio, S.P., Paixao, T.A., Butler, B.P., Chu, H., Santos, R.L., Berger, T., et al. (2009). Lipocalin-2 resistance confers an advantage to *Salmonella enterica* serotype *Typhimurium* for growth and survival in the inflamed intestine. *Cell Host Microbe* 5, 476–486.
- Richardson, A.R., Payne, E.C., Younger, N., Karlinsey, J.E., Thomas, V.C., Becker, L.A., Navarre, W.W., Castor, M.E., Libby, S.J., and Fang, F.C. (2011). Multiple targets of nitric oxide in the tricarboxylic acid cycle of *Salmonella enterica* serovar *typhimurium*. *Cell Host Microbe* 10, 33–43.
- Rivera-Chavez, F., Winter, S.E., Lopez, C.A., Xavier, M.N., Winter, M.G., Nuccio, S.P., Russell, J.M., Laughlin, R.C., Lawhon, S.D., Sterzenbach, T., et al. (2013). *Salmonella* uses energy taxis to benefit from intestinal inflammation. *PLoS Pathog.* 9, e1003267.
- Rivera-Chavez, F., Zhang, L.F., Faber, F., Lopez, C.A., Byndloss, M.X., Olsen, E.E., Xu, G., Velazquez, E.M., Lebrilla, C.B., Winter, S.E., et al. (2016). Depletion of butyrate-producing clostridia from the gut microbiota drives an aerobic luminal expansion of salmonella. *Cell Host Microbe* 19, 443–454.
- Rogowski, A., Briggs, J.A., Mortimer, J.C., Tryfona, T., Terrapon, N., Lowe, E.C., Basle, A., Morland, C., Day, A.M., Zheng, H., et al. (2015). Glycan complexity dictates microbial resource allocation in the large intestine. *Nat. Commun.* 6, 7481.
- Rubinstein, R., Howard, A.V., and Wrong, O.M. (1969). *In vivo* dialysis of faeces as a method of stool analysis. IV. The organic anion component. *Clin. Sci.* 37, 549–564.
- Schell, M.A., Karmirantzou, M., Snel, B., Vilanova, D., Berger, B., Pessi, G., Zwahlen, M.C., Desiere, F., Bork, P., Delley, M., et al. (2002). The genome sequence of *Bifidobacterium longum* reflects its adaptation to the human gastrointestinal tract. *Proc. Natl. Acad. Sci. USA* 99, 14422–14427.
- Schmieger, H. (1972). Phage P22-mutants with increased or decreased transduction abilities. *Mol. Gen. Genet.* 119, 75–88.
- Schwarz, W.H., Zverlov, V.V., and Bahl, H. (2004). Extracellular glycosyl hydrolases from clostridia. *Adv. Appl. Microbiol.* 56, 215–261.
- Shimizu, T., Ohtani, K., Hirakawa, H., Ohshima, K., Yamashita, A., Shiba, T., Ogasawara, N., Hattori, M., Kuwara, S., and Hayashi, H. (2002). Complete genome sequence of *Clostridium perfringens*, an anaerobic flesh-eater. *Proc. Natl. Acad. Sci. USA* 99, 996–1001.
- Simon, R., Priefer, U., and Puhler, A. (1983). A broad host range mobilization system for *in vivo* genetic engineering: transposon mutagenesis in gram negative bacteria. *Nat. Biotechnol.* 1, 784–791.

- Stecher, B., Barthel, M., Schlumberger, M.C., Haberli, L., Rabsch, W., Kremer, M., and Hardt, W.D. (2008). Motility allows *S. typhimurium* to benefit from the mucosal defence. *Cell Microbiol.* 10, 1166–1180.
- Stecher, B., Robbiani, R., Walker, A.W., Westendorf, A.M., Barthel, M., Kremer, M., Chaffron, S., Macpherson, A.J., Buer, J., Parkhill, J., et al. (2007). *Salmonella enterica* serovar *typhimurium* exploits inflammation to compete with the intestinal microbiota. *PLoS Biol.* 5, 2177–2189.
- Steeb, B., Claudi, B., Burton, N.A., Tienz, P., Schmidt, A., Farhan, H., Maze, A., and Bumann, D. (2013). Parallel exploitation of diverse host nutrients enhances *Salmonella* virulence. *PLoS Pathog.* 9, e1003301.
- Stojiljkovic, I., Baumler, A.J., and Heffron, F. (1995). Ethanolamine utilization in *Salmonella typhimurium*: nucleotide sequence, protein expression, and mutational analysis of the cchA cchB eutE eutJ eutG eutH gene cluster. *J. Bacteriol.* 177, 1357–1366.
- Tchawa Yimga, M., Leatham, M.P., Allen, J.H., Laux, D.C., Conway, T., and Cohen, P.S. (2006). Role of gluconeogenesis and the tricarboxylic acid cycle in the virulence of *Salmonella enterica* serovar *Typhimurium* in BALB/c mice. *Infect. Immun.* 74, 1130–1140.
- Thiennimitr, P., Winter, S.E., Winter, M.G., Xavier, M.N., Tolstikov, V., Huseby, D.L., Sterzenbach, T., Tsolis, R.M., Roth, J.R., and Baumler, A.J. (2011). Intestinal inflammation allows *Salmonella* to use ethanolamine to compete with the microbiota. *Proc. Natl. Acad. Sci. USA* 108, 17480–17485.
- Turton, L.J., Drucker, D.B., and Ganguli, L.A. (1983). Effect of glucose concentration in the growth medium upon neutral and acidic fermentation end-products of *Clostridium bifermentans*, *Clostridium sporogenes* and *Peptostreptococcus anaerobius*. *J. Med. Microbiol.* 16, 61–67.
- Unden, G., and Kleefeld, A. (2004). C4-dicarboxylate degradation in aerobic and anaerobic growth. EcoSal Plus 1, <http://dx.doi.org/10.1128/ecosalplus.3.4.5>.
- Vazquez-Baeza, Y., Pirrung, M., Gonzalez, A., and Knight, R. (2013). EMPeror: a tool for visualizing high-throughput microbial community data. *Gigascience* 2, 16.
- Wilson, R.P., Raffatellu, M., Chessa, D., Winter, S.E., Tukel, C., and Baumler, A.J. (2008). The Vi-capsule prevents Toll-like receptor 4 recognition of *Salmonella*. *Cell Microbiol.* 10, 876–890.
- Wimpenny, J.W., and Cole, J.A. (1967). The regulation of metabolism in facultative bacteria. 3. The effect of nitrate. *Biochim. Biophys. Acta* 148, 233–242.
- Winter, S.E., Thiennimitr, P., Nuccio, S.P., Haneda, T., Winter, M.G., Wilson, R.P., Russell, J.M., Henry, T., Tran, Q.T., Lawhon, S.D., et al. (2009). Contribution of flagellin pattern recognition to intestinal inflammation during *Salmonella enterica* serotype *typhimurium* infection. *Infect. Immun.* 77, 1904–1916.
- Winter, S.E., Thiennimitr, P., Winter, M.G., Butler, B.P., Huseby, D.L., Crawford, R.W., Russell, J.M., Bevins, C.L., Adams, L.G., Tsolis, R.M., et al. (2010). Gut inflammation provides a respiratory electron acceptor for *Salmonella*. *Nature* 467, 426–429.
- Winter, S.E., Winter, M.G., Poon, V., Keestra, A.M., Sterzenbach, T., Faber, F., Costa, L.F., Cassou, F., Costa, E.A., Alves, G.E., et al. (2014). *Salmonella enterica* Serovar Typhi conceals the invasion-associated type three secretion system from the innate immune system by gene regulation. *PLoS Pathog.* 10, e1004207.
- Winter, S.E., Winter, M.G., Xavier, M.N., Thiennimitr, P., Poon, V., Keestra, A.M., Laughlin, R.C., Gomez, G., Wu, J., Lawhon, S.D., et al. (2013). Host-derived nitrate boosts growth of *E. coli* in the inflamed gut. *Science* 339, 708–711.
- Wynosky-Dolfi, M.A., Snyder, A.G., Philip, N.H., Doonan, P.J., Poffenberger, M.C., Avizonis, D., Zwack, E.E., Riblett, A.M., Hu, B., Strowig, T., et al. (2014). Oxidative metabolism enables *Salmonella* evasion of the NLRP3 inflammasome. *J. Exp. Med.* 211, 653–668.
- Xu, J., Bjursell, M.K., Himrod, J., Deng, S., Carmichael, L.K., Chiang, H.C., Hooper, L.V., and Gordon, J.I. (2003). A genomic view of the human-*Bacteroides thetaiotaomicron* symbiosis. *Science* 299, 2074–2076.

STAR★METHODS

KEY RESOURCES TABLE

REAGENT or RESOURCE	SOURCE	IDENTIFIER
Antibodies		
Anti-rabbit alpha/beta-tubulin	Cell Signaling Technology	Cat# 2148S; RRID: AB_10693793
Anti-mouse iNOS	Becton Dickinson	Cat# 610431; RRID: AB_397807
Anti-rabbit peroxidase-conjugated	Bio-Rad Laboratories	Cat# 170-6515; RRID: AB_11125142
Anti-mouse peroxidase-conjugated	Bio-Rad Laboratories	Cat# 170-6516; RRID: AB_11125547
Bacterial and Virus Strains		
<i>E. coli</i> , DH5α λpir, <i>F</i> endA1 hsdR17 (<i>r</i> ⁻ <i>m</i> ⁺) supE44 thi-1 recA1 gyrA relA1 Δ(lacZYA-argF)U189 φ80lacZΔM15 λpir	Pal et al., 2005	DH5α λpir
<i>E. coli</i> , S17-1 λpir, zxx::RP4 2-(Tet ^R ::Mu) (Kan ^R ::Tn7) λpir recA1 thi pro hsdR (<i>r</i> ⁻ <i>m</i> ⁺)	Simon et al., 1983	S17-1 λpir
<i>S. Typhimurium</i> , IR715 ATCC14028 NaI ^R	Stojiljkovic et al., 1995	IR715
<i>S. Typhimurium</i> , SL1344 Strep ^R	Hoiseth and Stocker, 1981	SL1344
<i>S. Typhimurium</i> , IR715 phoN::Kan ^R	Kingsley et al., 2003	AJB715
<i>S. Typhimurium</i> , IR715 ΔinvA::Tet ^R ΔspiB::Kan ^R	Raffatellu et al., 2009	SPN452
<i>S. Typhimurium</i> , IR715 ΔinvA(-9 to +2057) ΔspiB(+25 to +1209)	Rivera-Chavez et al., 2013	SPN487
<i>S. Typhimurium</i> , ATCC14028 ΔsdhA::Kan ^R	Porwollik et al., 2014	STM0734
<i>S. Typhimurium</i> , SL1344 ΔsdhA	This study	MW156
<i>S. Typhimurium</i> , SL1344 ΔinvA::Tet ^R ΔspiB::Kan ^R	This study	MW231
<i>S. Typhimurium</i> , SL1344 ΔinvA::Tet ^R ΔspiB::Kan ^R phoN::Cm ^R	This study	MW251
<i>S. Typhimurium</i> , SL1344 ΔinvA::Tet ^R ΔspiB::Kan ^R ΔsdhA	This study	MW256
<i>S. Typhimurium</i> , SL1344 phoN::Cm ^R	Winter et al., 2014	SW759
<i>S. Typhimurium</i> , IR715 ΔsdhA ::Kan ^R	This study	SW1056
<i>S. Typhimurium</i> , IR715 ΔinvA ΔspiB ΔsdhA::Kan ^R	This study	SW1203
<i>S. Typhimurium</i> , IR715 ΔsucAB	This study	SW1285
<i>S. Typhimurium</i> , IR715 ΔsucCD	This study	SW1286
<i>S. Typhimurium</i> , IR715 ΔaceAB	This study	SW1288
<i>S. Typhimurium</i> , IR715 ΔsdhA	This study	SW1397
<i>S. Typhimurium</i> , IR715 ΔinvA ΔspiB phoN::Kan ^R	This study	SW1401
<i>S. Typhimurium</i> , IR715 ΔsdhA phoN::sdhA	This study	SW1410
<i>S. Typhimurium</i> , IR715 ΔdcuA ΔdcuB ΔdctA ΔsdhA::Kan ^R	This study	SW1411 (Δ3)
<i>S. Typhimurium</i> , IR715 ΔdcuA ΔdcuB ΔdctA ΔsdhA::Kan ^R	This study	SW1413
<i>S. Typhimurium</i> , IR715 ΔsdhA phoN::Kan ^R	This study	SW1414
<i>B. thetaiotaomicron</i> , VPI 5482 Δtdk	Koropatkin et al., 2008	VPI 5482 Δtdk
<i>B. thetaiotaomicron</i> , Δtdk ΔfrdCAB	This study	MW399
Chemicals, Peptides, and Recombinant Proteins		
Gibson Assembly Master Mix	NEB	Cat# E2611L
LB Broth, Miller (Luria Bertani)	Becton Dickinson	Cat# 244520
LB Agar, Miller (Luria Bertani)	Becton Dickinson	Cat# 244620
Bacto Brain Heart Infusion	Becton Dickinson	Cat# 237500
Sheep Blood	Hemostat	Cat# DSB1
Columbia Agar	Sigma	Cat# 27688
Bacto Tryptone	Becton Dickinson	Cat# 211705
Sodium Nitrate	Sigma	Cat# S5506
Sodium Tetraphionate	Sigma	Cat# P2926
5-fluoro-2'-deoxyuridine (FUdR)	ARK Pharm	Cat# AK-24802-1

(Continued on next page)

Continued

REAGENT or RESOURCE	SOURCE	IDENTIFIER
Mucin from porcine stomach, Type II	Sigma-Aldrich	Cat# M2378
TRI Reagent	Molecular Research	Cat# TR118
TaqMan Reverse Transcription Reagents	Life Technologies	Cat# N8080234
SYBR Green qPCR Master Mix	Life Technologies	Cat# 4309155
Succinic-2,2,3,3,-d ₄ acid	CDN Isotopes	Cat# D-197
Pyridine anhydrous	Sigma	Cat# 270970
MTBSTFA (with 1% t-BDMCS)	Sigma	Cat# M-108
Critical Commercial Assays		
Succinic acid enzymatic assay	Megazyme	Cat# K-SUCC
Aurum Total RNA Mini Kit	BioRad	Cat# 7326820
PowerMicrobiome RNA Isolation Kit	MoBio	Cat# 26000-50
RNeasy Purification kit	Qiagen	Cat# 74204
TruSeq Stranded Total RNA Library Prep kit	Illumina	Cat# RS-122-2201
Tributyrin	Sigma	Cat# W222305
Immobilon Western Chemiluminescent HRP Substrate	Millipore	Cat# WBKLS0500
Deposited Data		
<i>Salmonella</i> <i>in vivo</i> RNAseq dataset	European Nucleotide Archive	PRJEB21324
<i>Salmonella</i> transcriptomic compendium from Kroger et al., 2013 (http://bioinf.gen.tcd.ie/cgi-bin/salcom.pl?_HL)	GEO database	GSE49829
Experimental Models: Organisms/Strains		
C57BL/6 WT	Jackson Laboratory	Cat# 000664
C57BL/6 Cybb ^{-/-}	Jackson Laboratory	Cat# 002365
C57BL/6 Nos2 ^{-/-}	Jackson Laboratory	Cat# 002609
CBA/J	Jackson Laboratory	Cat# 000656
Swiss Webster, ex Germ-Free colonized with CBA/J microbiota	This study	N/A
Germ-free Swiss-Webster	Hooper Lab	N/A
Oligonucleotides		
Primer used in this study, see Table S1	This paper	N/A
Recombinant DNA		
Plasmid: pExchange-tdk, ori(R6K) mobRP4 tdk Carb ^R Erm ^R	Koropatkin et al., 2008	pExchange-tdk
Plasmid: pGP704, ori(R6K) mobRP4 Carb ^R	Miller and Mekalanos, 1988	pGP704
Plasmid: pRDH10, ori(R6K) mobRP4 sacRB Cm ^R Tet ^R	Kingsley et al., 1999	pRDH10
Plasmid: Up- and downstream region of sucAB in pRDH10	This study	pSW284
Plasmid: Up- and downstream region of succD in pRDH10	This study	pSW286
Plasmid: Up- and downstream region of aceAB in pRDH10	This study	pSW288
Plasmid: Up- and downstream region of sdhA in pRDH10	This study	pSW306
Plasmid: Internal fragment of the phoN coding sequence cloned into pGP704	This study	pSW327
Plasmid: sdhA promoter and coding sequence cloned into pSW327	This study	pSW328
Plasmid: Up- and downstream region of dctA in pRDH10	This study	pSW299
Plasmid: Up- and downstream region of dcuA in pRDH10	This study	pSW300
Plasmid: Up- and downstream region of dcuB in pRDH10	This study	pSW301
Plasmid: Up- and downstream region of frdCAB in pExchange-tdk	This study	pMW5
Software and Algorithms		
Prism 7	GrapPad Software	https://www.graphpad.com/scientific-software/prism/
TapeStation 4200	Agilent, CA	

(Continued on next page)

Continued

REAGENT or RESOURCE	SOURCE	IDENTIFIER
BBmap software suite		http://jgi.doe.gov/data-and-tools/bbtools/
Bowtie2	Langmead and Salzberg, 2012	http://bowtie-bio.sourceforge.net/bowtie2/index.shtml
R Vegan		https://cran.r-project.org/web/packages/vegan/index.html
Qiime	Caporaso et al., 2010	http://qiime.org
Emperor	Vazquez-Baeza et al., 2013	https://biocore.github.io/emperor/
GCMS Real Time Analysis	Shimadzu, TQ8040	N/A
Photoshop CS6	Adobe Photoshop	N/A
G:Box Imaging System	Syngene	N/A

CONTACT FOR REAGENT AND RESOURCE SHARING

Further information and requests for resources and reagents should be directed to and will be fulfilled by the Lead Contact, Sebastian E. Winter (Sebastian.Winter@UTSouthwestern.edu).

EXPERIMENTAL MODEL AND SUBJECT DETAILS**Mice**

C57BL/6, *Cybb*-deficient (on the C57BL/6 background), *Nos2*-deficient (on the C57BL/6 background) and CBA mice were originally obtained from the Jackson Laboratory and bred at UT Southwestern. Germ-free Swiss Webster mice were maintained in specific pathogen-free facilities at UT Southwestern Medical Center. Some of the germ-free mice were colonized with CBA mice microbiota to obtain the Swiss Webster mice used in this study. Conventional mice were housed in individually ventilated cages with *ad libitum* access to water and feed (Envigo Global 16% Protein Rodent Diet). The age at the begin of the experiment was 7-10 weeks for C57BL/6 WT, *Cybb*, and *Nos2*-deficient mice, 8-10 weeks for CBA mice, and 6-8 weeks for Swiss Webster mice. Unless indicated otherwise in the figure legend, both male and female mice were analyzed and no significant sex-specific differences were noted. Both sexes were equally represented in each experimental group.

Animals were randomly assigned into cages and treatment groups 3 days prior to experimentation. Unless stated otherwise, a minimum of 5 mice were used based on variability observed in previous experiments. At the end of the experiments, mice were humanely euthanized using carbon dioxide inhalation. Animals that had to be euthanized for humane reasons prior to reaching the predetermined time point were excluded from the analysis. All experiments involving mice were approved by the Institutional Animal Care and Use Committee at UT Southwestern Medical Center (APN# T-2013-0139, T2014-0061, T-2015-0031).

Bacterial Culture

E. coli and *S. Tm* strains were routinely grown aerobically at 37°C in LB broth (10 g/l tryptone, 5 g/l yeast extract, 10 g/l sodium chloride) or on LB agar plates (10 g/l tryptone, 5 g/l yeast extract, 10 g/l sodium chloride, 15 g/l agar). *B. thetaiotaomicron* strains were routinely cultured on blood agar plates (37 g/l brain heart infusion medium, 15 g/l agar, 50 ml sheep blood, 50 mg/l glutamine), Columbia blood plates (42 g/l Columbia agar, 5 % [v/v] defibrinated blood, 5 mg/l hemin, 0.02% [v/v] of a 0.5 % [v/v] Vitamin K1 solution in 95 % ethanol), or in modified TYG broth (10 g/l tryptone, 5 g/l yeast extract, 2 g/l glucose, 0.5 g/l cysteine 0.1 M potassium phosphate pH 7.2, 1 mg/l Vitamin K, 0.02 g/l magnesium sulfate heptahydrate, 0.4 g/l sodium bicarbonate, 0.08 g/l sodium chloride, 8 mg/l calcium chloride, 0.4 mg/l iron (II) sulfate, 1 mg/l resazurin, 40 μM histidine, 2.4 μg/l hematin) in an anaerobic chamber (Sheldon Manufacturing; 5 mol % H₂, 5 % CO₂, 90 % N₂). When appropriate, agar plates and media were supplemented with 30 μg/ml chloramphenicol (Cm), 100 μg/ml carbenicillin (Carb), 50 μg/ml kanamycin (Kan), 50 μg/ml nalidixic acid (Nal), 50 μg/ml gentamycin (Gent), 25 μg/ml erythromycin (Erm), 25 μg/ml tetracycline (Tet) or 200 μg/ml 5-fluoro-2'-deoxyuridine (FUdR). For competitive growth assays, diluted samples were spread onto agar plates containing the chromogenic substrate 5-bromo-4-chloro-3-indolyl phosphate (40 mg/l) to detect acidic phosphatase (PhoN) activity. The competitive index was calculated by dividing the number of wild-type bacteria by the number of mutant bacteria in the output, divided by the same ratio obtained from the inoculum.

METHOD DETAILS**Construction of Plasmids**

To generate pSW284, pSW286 and pSW288, the upstream and downstream regions of *S. Tm* IR715 *sucAB*, *sucCD* and *aceAB* were amplified by PCR using the primer sets listed in the table below. Purified PCR products were digested with XbaI and ligated

with T4 DNA ligase. The joint upstream and downstream regions were then amplified by PCR using the outside primers and cloned into pCR2.1. The DNA sequence of the cloned PCR product was verified by Sanger sequencing. The DNA fragment was subcloned into pRDH10 using BamHI and SalI restriction sites. To construct pSW306, pSW300, pSW301, and pSW299, the upstream regions of *sdhA*, *dcuA* *dcuB*, and *dctA* were PCR amplified from the IR715 chromosome. Purified PCR products and purified, SphI-digested pRDH10 were ligated using the Gibson cloning procedure in a three-part ligation. The DNA sequence of the upstream and downstream region was determined sequencing. For pSW328, an internal fragment of the *phoN* coding sequence was amplified by PCR and cloned into SacI-digested pGP704 in a Gibson cloning reaction. Subsequently, the promoter and coding sequence of the *S. Tm* *sdh* operon were amplified and cloned into the SphI restriction enzyme site of pSW327. To generate pMW5, regions upstream and downstream of *frdCAB* in *B. thetaiotaomicron* were PCR amplified and the products were inserted into the BamHI site of the suicide vector pExchange-tdk through Gibson assembly. The cloning strain for all suicide plasmids was DH5 α λ pir.

Generation of *S. Tm* Mutants

Suicide plasmids were introduced into *S. Tm* by conjugation using S17-1 λ pir as the donor strain. For pRDH10 and pGP704 derivatives, Cm and Carb, respectively were used to select for single cross over events. To select for a second crossover event, sucrose selection was performed (Lawes and Maloy, 1995). pSW306, pSW284, pSW286, pSW288 were used to generate SW1397, SW1285, SW1286, SW1288 in the IR715 background and to generate MW156 in the SL1344 background, respectively. pSW328 was integrated into SW1397 to give rise to SW1410. Integration of pSW328 into the *phoN* gene was confirmed by PCR and lack of acidic phosphatase activity. SW1411 was generated by sequential introduction of pSW299, pSW300, and pSW301 into IR715 followed each time by sucrose selection. The *phoN*::Kan^R mutation was transduced by phage P22 HT int-105 (Schmieger, 1972) from AJB715 into SPN487 and SW1397 to generate SW1401 and SW1414, respectively. Similarly, the *AsdhA*::Kan^R from STM0734 was introduced into IR715, SPN487 and SW1411, thus generating SW1056, SW1203 and SW1413, respectively. To create MW231, the *ΔinvA*::Tet^R and *ΔspiB*::Kan^R mutations from SPN452 were transduced separately. Introduction of *phoN*::Cmr and pSW306 into MW231 produced MW251 and MW256, respectively.

Construction of a *B. thetaiotaomicron* *frd* Mutant

MW399, an isogenic derivative of the *B. thetaiotaomicron* strain ATCC 29148 *Δtdk* deficient for *frdCAB*, was generated via allelic exchange (Koropatkin et al., 2008). pMW5 was introduced into ATCC 29148 *Δtdk* via bacterial conjugation with the donor strain S17-1 λ pir. The conjugation was carried out on blood plates under aerobic conditions at 37°C to enable the growth of the S17-1 λ pir strain. All further steps were performed under anaerobic conditions to insure proper growth of the *B. thetaiotaomicron* strains. Exconjugates in which the suicide plasmid had integrated into the chromosome by single crossover were selected for on blood plates containing Gent and Erm. Then, the second homologous recombination event was selected for on blood plates containing FUdR. The second crossover event leads to an unmarked deletion of *frdCAB*, which was confirmed by PCR. The growth media was routinely supplemented with hemin.

Growth of *B. thetaiotaomicron* in Mucin Broth

Porcine mucin was sterilized by suspending 100 mg in 1 ml of 70 % ethanol for 24 h. The ethanol was removed by drying in a vacuum concentrator. Sterile mucin was dissolved in No-Carbon E medium (NCE) (3.94 g/l monopotassium phosphate, 5.9 g/l dipotassium phosphate, 4.68 g/l ammonium sodium hydrogen phosphate tetrahydrate, 2.46 g/l magnesium sulfate heptahydrate) at a final concentration of 0.5 % (w/v). Mucin broth was inoculated with a fresh colony of *B. thetaiotaomicron* and incubated under anaerobic conditions for 72 h at 37°C. Digested mucin broth was filter-sterilized (0.5 μ m pore size).

Succinate Concentration Measurement in Digested Mucin

The succinate concentration in digested mucin was measured using a coupled enzymatic assay according to the recommendations of the manufacturer. Freshly prepared solutions of pure succinate were used as a standard curve. Some biological samples were spiked with known amounts of pure succinate as controls.

Anaerobic Growth of *S. Tm* in Mucin Broth

Fresh hog mucin broth (0.5 % mucin in NCE media) or filter-sterilized supernatant of *B. thetaiotaomicron*-digested mucin was inoculated with equal mixtures of the *S. Tm* *phoN* mutant (wild-type strain; AJB715) and the *AsdhA* mutant (SW1397), the *ΔsucAB* mutant (SW1285), the *ΔsucCD* mutant (SW1286), and the *ΔdcuA* *ΔdcuB* *ΔdctA* mutant (SW1411) or the *AsdhA* *phoN*::Kan^R mutant (SW1414) and the *AsdhA* *ΔdcuA* *ΔdcuB* *ΔdctA* mutant (SW1413) at a final concentration of 1 \times 10³ CFU/ml for each strain. Sodium nitrate or sodium tetrathionate were added at a final concentration of 40 mM, as indicated. After 18 h of anaerobic growth at 37°C, bacterial numbers were determined by spreading serial ten-fold dilutions on selective LB agar plates.

Animal Models of *S. Tm*-Induced Colitis

Streptomycin-Treated Mouse Model

Groups of 7-10 week old C57BL/6 mice received 20 mg per animal through the intragastric route. After 24 h, mice were intragastrically inoculated with 1 \times 10⁹ CFU for single strain infection experiments, 5 \times 10⁸ CFU of each strain for competitive infection

experiments, or mock treated (LB broth). For the experiments shown in [Figure 1](#), groups of mice were infected with equal mixtures of A JB715 and SW1056 as well as SW1401 and SW1203. For the experiments shown in [Figure 2](#), groups of animals were infected with IR715 or SPN487. For the experiments shown in [Figure 3](#), groups of mice were infected with equal mixtures of A JB715 and SW1397. In some experiments, animals were orally treated with tributyrin (5 g/kg) 3 h post infection or mock-treated with PBS ([Rivera-Chavez et al., 2016](#)). Two, three, and four days after infection, samples for histopathology, flash frozen cecal and colonic tissue for RNA and protein extraction, and cecal and colonic luminal material (S. Tm colonization) were collected, as indicated. In some experiments, luminal content was flash frozen (liquid nitrogen) for bacterial gene expression analyses.

CBA Colitis Model

Groups of 8–10 week old CBA mice were intragastrically infected with 1×10^9 CFU for single strain infection experiments, 5×10^8 CFU of each strain for competitive infection experiments, or mock treated (LB broth). After 7 days, samples were collected as described above. For the experiments shown in [Figures 4A](#) and [4B](#), mice were infected with A JB715 and SW1285, A JB715 and SW1286, A JB715 and SW1288, A JB715 and SW1056, SW1401 and SW1203, SW1410 and SW1397, respectively. For the experiments shown in [Figures 4C–4F](#), groups of animals were inoculated with IR715 and SW1397, respectively. For [Figures 5A–5C](#), groups of animals were infected with A JB715 and SW1397, A JB715 and SW1411, or SW1410 and SW1413. For [Figures 5C–5E](#), groups of animals were infected with IR715, SW1411, or mock-treated.

Germ-Free and Conventionally-Raised Swiss Webster Mice

6–8 week old germ-free mice were intragastrically inoculated with 3×10^9 CFU of *B. thetaiotaomicron*. After 3 days, mono-associated and germ-free control animals were infected with an equal mixture of A JB715 and SW1411, SW1410 and SW1413, or A JB715 and SW1397 as described above. Furthermore, cecal microbiota from one CBA donor mouse was orally transferred to a germ-free Swiss Webster breeder pair, which was then maintained under conventional housing conditions. Offspring from this breeder pair was used for the experiment shown in [Figure S5C](#).

Quantification of Inflammatory Markers by qRT-PCR

Relative mRNA levels of *Nos2*, *Cxcl1*, and *Tnfa* was determined by qRT-PCR as described previously ([Winter et al., 2009](#)). Briefly, tissue was homogenized in a Mini beadbeater (Biospec Products) and RNA was extracted using the TRI reagent method. cDNA was generated by TaqMan reverse transcription reagents. Real-time PCR was performed using SYBR Green qPCR master mix. Data was acquired in a QuantStudio 6 Flex instrument (Life Technologies) and analyzed using the comparative Ct method. Target gene transcription of each sample was normalized to *Gapdh* mRNA levels.

Bacterial Gene Expression

To determine bacterial gene expression *in vitro*, mucin broth was inoculated with 1×10^3 CFU/ml of S. Tm and anaerobically cultured at 37°C for 16 h. Sodium nitrate and tetrathionate was added at a concentration of 40 mM, as indicated. RNA was extracted using the Aurum Total RNA Mini Kit. To investigate bacterial gene expression in the intestinal content, flash frozen cecal material in TRI reagent was homogenized for 1 min in a bead beater (BioSpec) and RNA isolated using the TRI reagent method. RT-PCR and qPCR were performed as described above. Gene expression was normalized to S. Tm 16S rRNA levels. A mock-RT-PCR, lacking reverse transcriptase, was performed for each sample and gene of interest to control for DNA contamination.

Histopathology

Cecal and colonic tissue was fixed in phosphate-buffered formalin for 48 h and embedded in paraffin. Sections (5 μm) were stained with hematoxylin and eosin. Stained sections were blinded and evaluated by a veterinary pathologist according to the criteria listed in the [Supplemental Information](#). The contrast for the images was uniformly (linear) adjusted using Photoshop CS6.

iNOS Expression in Intestinal Tissue by Western Blot

After murine colonic tissue homogenization with a Mini-BeadBeater (BioSpec Products), colonic proteins were extracted with TRI Reagent according to the manufacturer's specifications (Molecular Research Center). Precipitated proteins were resuspended in a 1 % w/v sodium dodecyl sulfate (SDS) and 10 mM β-mercaptoethanol solution. Protein concentration of each sample was calculated based on the absorbance at 280 nm measured with an Epoch Microplate Spectrophotometer (BioTek Instruments). Samples were boiled for 1 min and then 10 μg of each sample were resolved by 10% SDS-PAGE. Proteins were transferred to polyvinylidene fluoride (PVDF) membranes (Millipore Immobilon-P) by wet transfer (Bio-Rad Laboratories). Membranes were blocked in 3 % non-fat dry milk and 0.1 % Tween 20 in phosphate-buffered saline (pH 7.4) solution. To detect tubulin and inducible nitric oxide synthase (iNOS) expression, membranes were incubated overnight with primary antibodies. Horseradish peroxidase-conjugated antibodies were used as secondary antibodies. A G:Box imaging system (Syngene) was used to detect the secondary antibodies after 1 min incubation with Immobilon Western Substrate. Images were processed with Photoshop CS6 (Adobe) to uniformly adjust brightness levels.

Metabolite Profiling and Quantification of Succinate

Colon and cecal content from mice was collected in sterile PBS. Samples were agitated for 2 min and debris and bacterial cells were removed by centrifugation at 6,000 g for 15 min at 4°C. For *in vitro* bacterial cultures, 2 ml of culture were centrifuged at 20,000 g at 4°C. The supernatant was removed and succinic-2,2,3,3-d₄ acid was added as an internal control. Samples were dried using a

SpeedVac concentrator (Eppendorf) for 2 h and stored at -80°C. External standards and biological samples were derivatized as follows: After adding 0.1 ml of water-free pyridine, each sample was sonicated for 1 min and incubated for 20 min at 80°C. Then 0.1 ml of *N*-*tert*-Butyldimethylsilyl-*N*-methyltrifluoroacetamide with 1 % *tert*-Butyldimethylchlorosilane was added to the samples and incubated at 80°C for 1 h. After centrifugation at 20,000 g, derivatized samples were transferred to autosampler vials for gas chromatography-mass spectrometry (GC-MS) analysis (Shimadzu, TQ8040). The injection temperature was 250°C and the injection split ratio was set to 1:50 with an injection volume of 1 µl. The oven temperature started at 50°C for 2 min, increasing to 100°C at 20°C per min and to 330°C at 40°C per min with a final hold at this temperature for 3 min. Flow rate of the helium carrier gas was kept constant at a linear velocity of 50 cm/s. The column used was a 30 m × 0.25 mm × 0.25 µm Rtx-5Sil MS (Shimadzu). The interface temperature was 300°C. The electron impact ion source temperature was 200°C, with 70 V ionization voltage and 150 µA current. For qualitative experiments, Q3 scans (range of 50–550 m/z, 1000 m/z per second) were performed. The retention time for succinate and deuterated succinate was 10.877 and 10.868 minutes respectively. Multiple reaction monitoring mode was used to quantitatively measure succinate and deuterated succinate, target ion m/z 289>147 reference ion m/z 331>189, and target ion m/z 293>147 reference ion m/z 335>189, respectively.

Transcriptional Profile of *S. Tm* in the Large Intestine

Gnotobiotic Swiss Webster mice were orally inoculated with 1×10^5 CFU of AJB715 for 48 h as described above. Cecal content was collected and stored in RNAlater at -80°C until further processing. Total RNA was extracted and cleaned using RNeasy PowerMicrobiome kit and RNeasy Purification kit (Qiagen, MD) according to the recommendations of the manufacturer. RNAseq library was constructed using TruSeq Stranded Total RNA Library Prep kit (Illumina, CA) and the resulting cDNA library was analyzed using TapeStation 4200 (Agilent, CA). Single-end 150 bp sequencing was conducted on an Illumina NextSeq system (Illumina, CA). RNAseq reads were trimmed and decontaminated using BBmap software suite. Reads that failed to align to mouse genome were mapped to the *S. Tm* LT2 genome using Bowtie2 ([Langmead and Salzberg, 2012](#)). Number of reads of each gene was determined using the Subread package ([Liao et al., 2014](#)). Relative expression of genes was determined, grouped into indicated pathways, and compared to previously published data ([Kroger et al., 2013](#)). The Bray-Curtis distances between samples was calculated using R Vegan packages implemented through Qiime ([Caporaso et al., 2010](#)) and visualized via Emperor ([Vazquez-Baeza et al., 2013](#)). The RNAseq dataset was deposited at the European Nucleotide Archive under accession number PRJEB21324.

QUANTIFICATION AND STATISTICAL ANALYSIS

Statistical Analysis

Statistical data analysis was performed using Graphpad PRISM. Succinate concentrations, fold changes in mRNA transcription, competitive indices, and abundance of *Salmonella* (CFU/g) underwent logarithmic transformation prior to descriptive and inferential statistical analysis. All transformed data was normally distributed, as determined by D'Agostino-Pearson normality test for large group sizes and Shapiro-Wilk for smaller sizes. The statistical significance of differences between groups was determined using the parametric Student's *t*-test applied to the log-transformed, normally distributed data. Cumulative histopathology scores did not follow a normal distribution and thus were analyzed using the non-parametric Mann-Whitney *U* test. Unless indicated otherwise, * $P < 0.05$; ** $P < 0.01$; *** $P < 0.001$; and ns, not statistically significant. Unless indicated otherwise in the figure legend, bars represent the geometric mean +/- standard error. When displaying aggregate data from mouse experiments, the number of animals per group (N) is indicated above each graph or in the figure legend. Animals that had to be euthanized for humane reasons prior to reaching the predetermined time point were excluded from the analysis.

DATA AND SOFTWARE AVAILABILITY

The accession number for the RNAseq data reported in this paper is European Nucleotide Archive: PRJEB21324.

Supplemental Information

An Oxidative Central Metabolism Enables *Salmonella* to Utilize Microbiota-Derived Succinate

Luisella Spiga, Maria G. Winter, Tatiane Furtado de Carvalho, Wenhan Zhu, Elizabeth R. Hughes, Caroline C. Gillis, Cassie L. Behrendt, Jiwoong Kim, Daniela Chessa, Helene L. Andrews-Polymeris, Daniel P. Beiting, Renato L. Santos, Lora V. Hooper, and Sebastian E. Winter

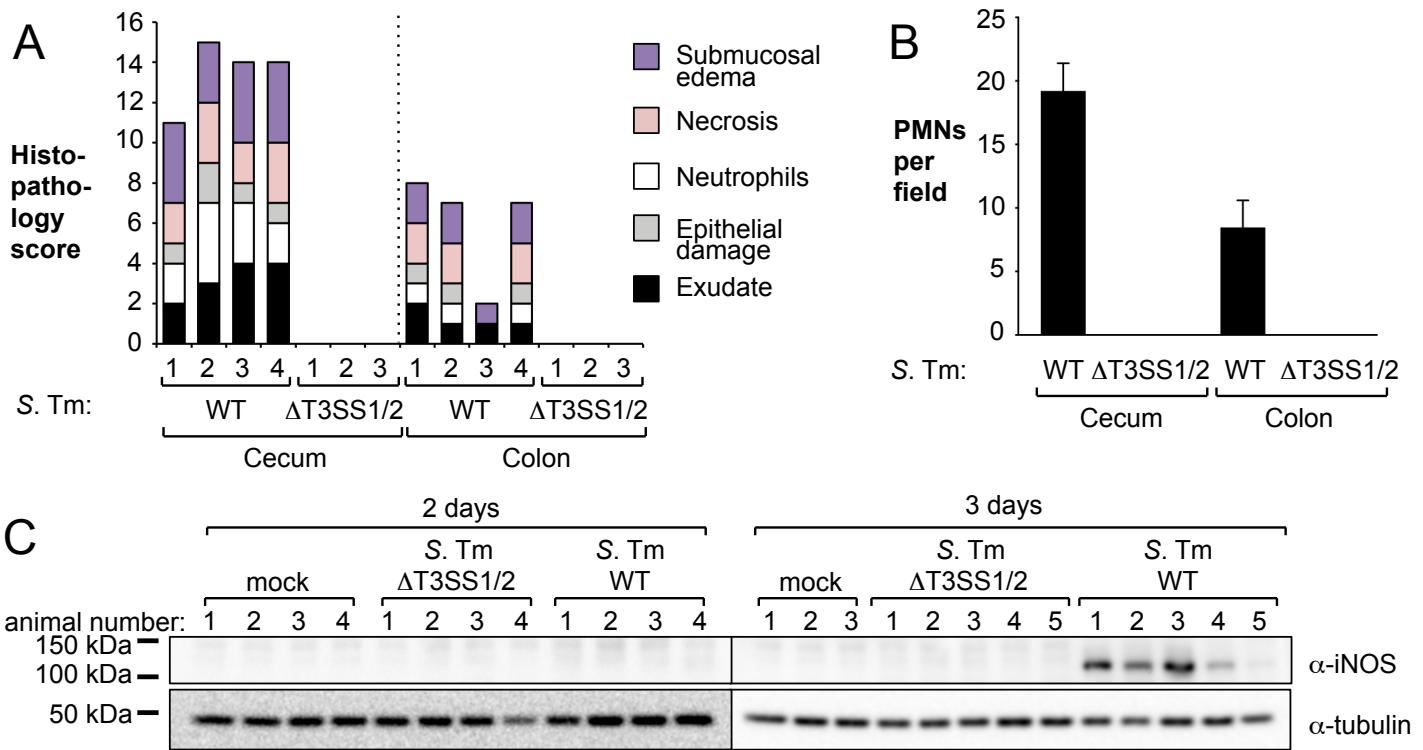


Figure S1: *Salmonella* induces large intestinal inflammation in the streptomycin-treated mouse model. Related to Fig. 1. (A – C) Groups of streptomycin-pretreated C57BL/6 mice were intragastrically inoculated with the *S. Tm* IR715 wild-type strain (WT), an isogenic $\Delta T3SS1/2$ ($\Delta invA \Delta spiB$) mutant, or mock-treated with LB. (A) Semi-quantitative histopathology score for the cecum and the colon tissue 4 days after infection. Each bar represents one animal. (B) Infiltration of the cecal and colonic mucosa with PMNs 4 days after infection. A total number of 10 fields were counted per individual animal. Bars represent the mean \pm standard error. (C) Colonic tissue samples, obtained 2 and 3 days after infection, were lysed and analyzed by western blot to detect expression of iNOS and tubulin (loading control). The approximate molecular mass is indicated on the left. Each lane represents one animal.

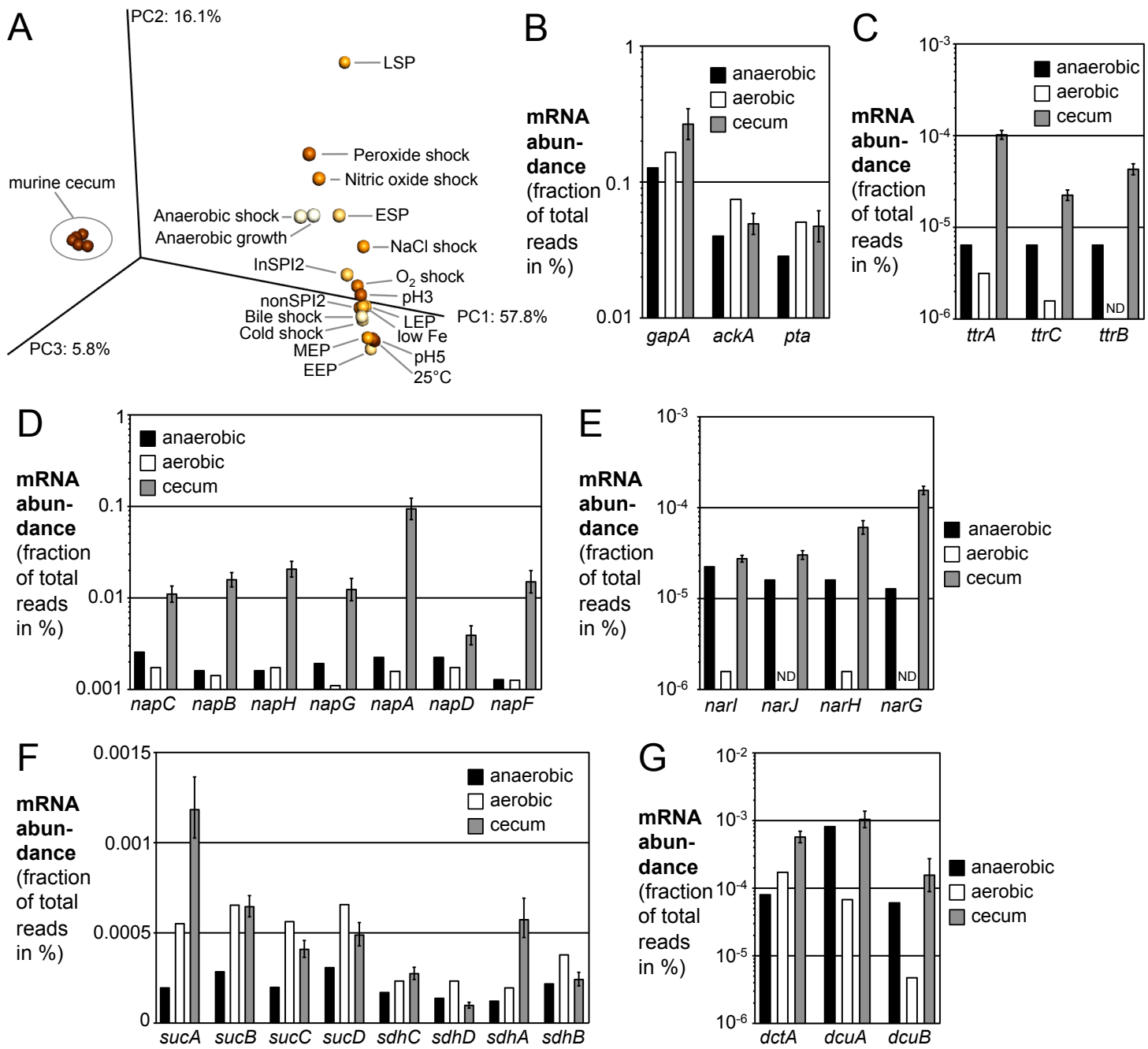


Figure S2: *Salmonella* transcriptome analysis. Related to Fig. 2. Five gnotobiotic mice were intragastrically inoculated with the *S. Typhimurium* wild-type strain. Two days after infection, total RNA was extracted from the cecal content and RNAseq performed. This *in vivo* transcriptome was compared to a published database (Kroger *et al.*, 2013). (A) Principal coordinate analysis plot comparing the overall transcriptome of *S. Typhimurium* in various *in vitro* growth conditions. EEP, early exponential phase; MEP, middle exponential phase; LEP, late exponential phase; ESP, early stationary phase; LSP, late stationary phase; low Fe, iron starvation. For details see Kroger *et al.*, 2013. (B – G) Relative transcription of “housekeeping” enzymes (B), tetrathionate reductase (C), periplasmic nitrate reductase (D), nitrate reductase 1 (E), α -ketoglutarate dehydrogenase, succinyl-CoA synthetase, and succinate dehydrogenase (F) and C4-dicarboxylate carriers under anaerobic (black bars) and aerobic (white bars) *in vitro* conditions (Kroger *et al.*, 2013) as well as the murine cecum (gray bars).

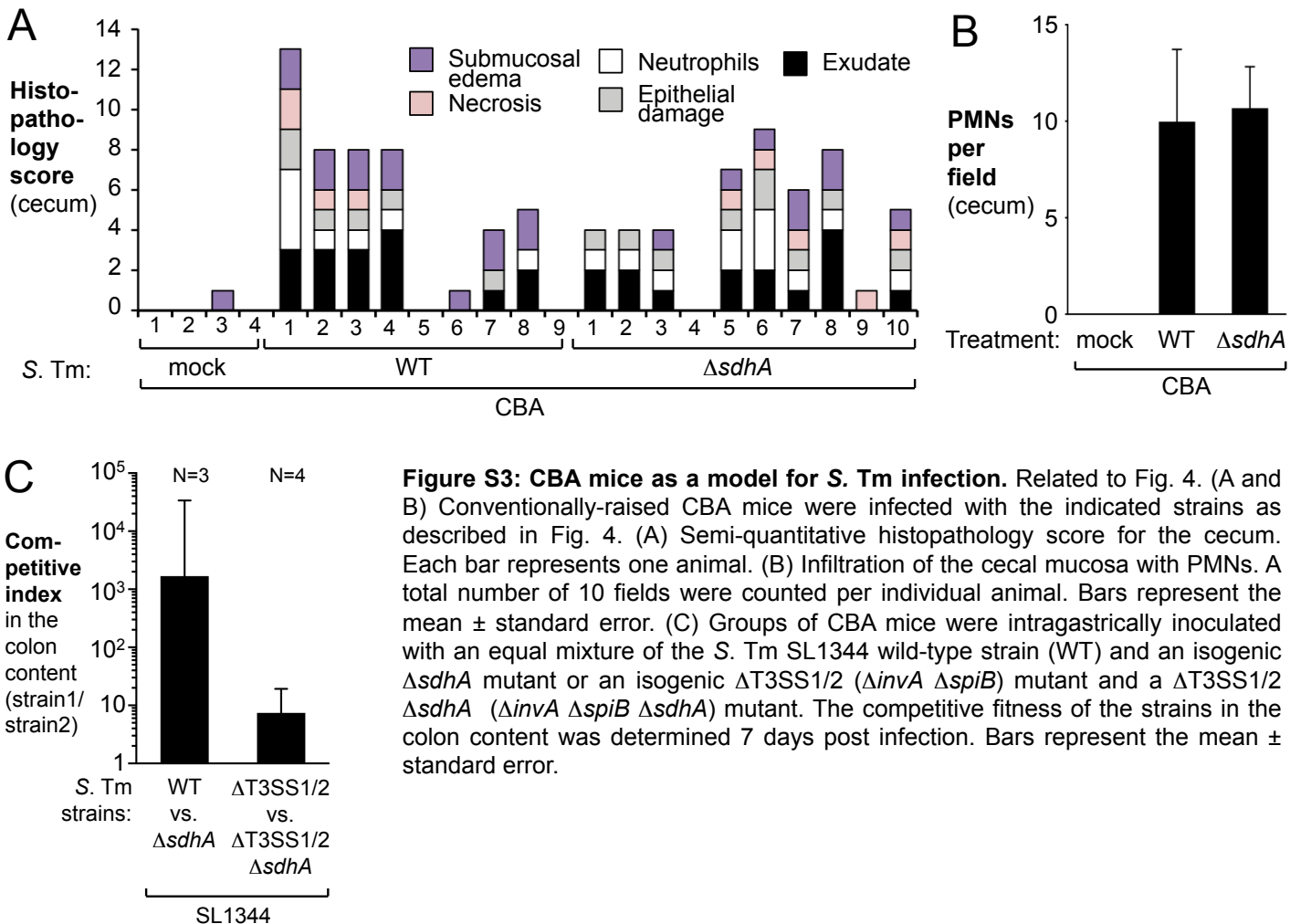


Figure S3: CBA mice as a model for S. Tm infection. Related to Fig. 4. (A and B) Conventionally-raised CBA mice were infected with the indicated strains as described in Fig. 4. (A) Semi-quantitative histopathology score for the cecum. Each bar represents one animal. (B) Infiltration of the cecal mucosa with PMNs. A total number of 10 fields were counted per individual animal. Bars represent the mean \pm standard error. (C) Groups of CBA mice were intragastrically inoculated with an equal mixture of the S. Tm SL1344 wild-type strain (WT) and an isogenic Δ sdhA mutant or an isogenic Δ T3SS1/2 (Δ invA Δ spiB) mutant and a Δ T3SS1/2 Δ sdhA (Δ invA Δ spiB Δ sdhA) mutant. The competitive fitness of the strains in the colon content was determined 7 days post infection. Bars represent the mean \pm standard error.

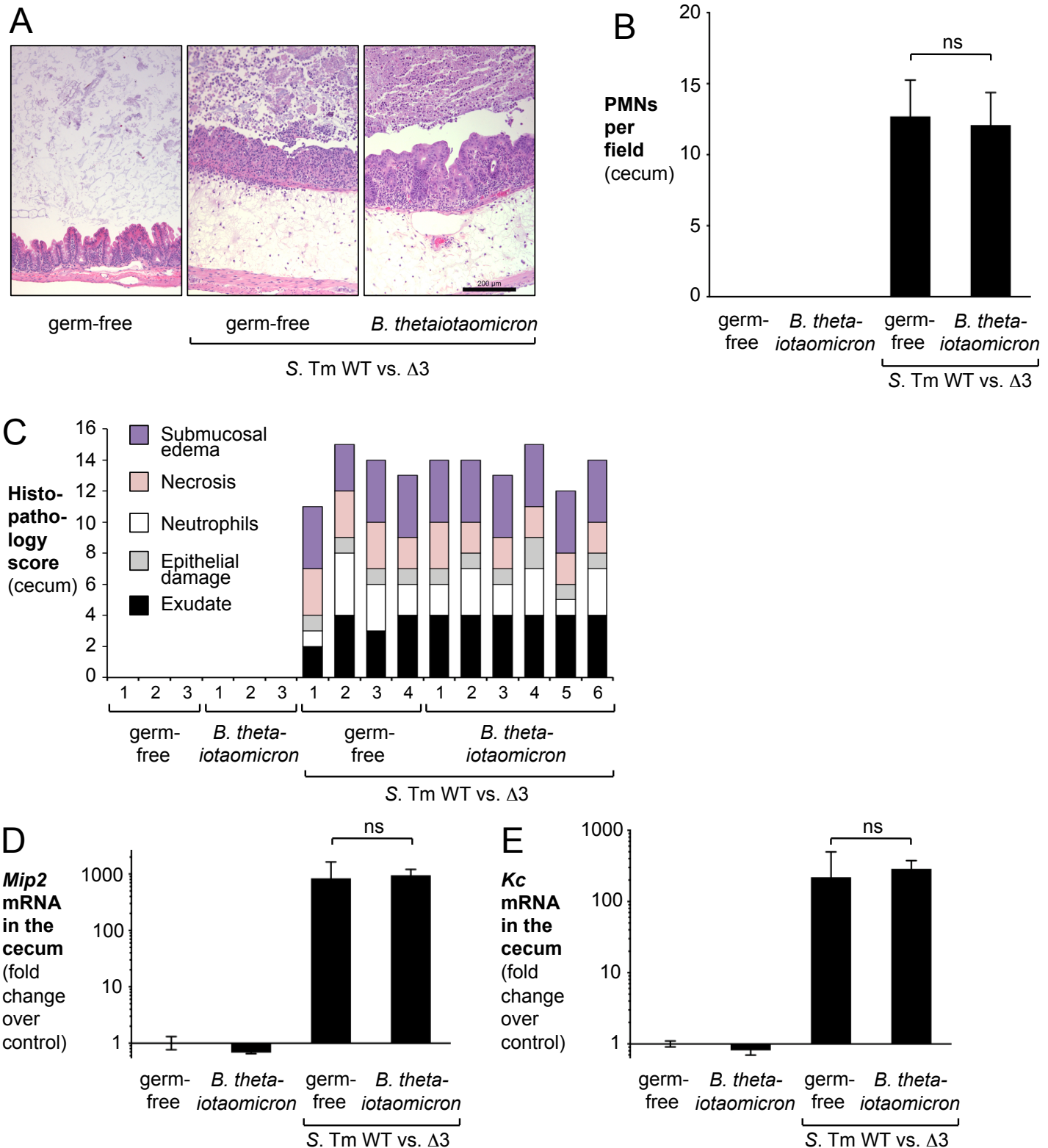


Figure S4: Cecal inflammation induced by S. Tm in a gnotobiotic mouse model. Related to Fig. 6. Germ-free animals and mice mono-associated with *B. thetaiotaomicron* were mock-treated or infected with S. Tm as shown in Fig. 6 and cecal inflammation analyzed. (A) Representative images of hematoxylin and eosin-stained sections. (B) Infiltration of the cecal mucosa with PMNs. A total number of 10 fields were counted per individual animal. Bars represent the mean \pm standard error. ns, not statistically significant. (C) Semi-quantitative histopathology score for the cecum. Each bar represents one animal. (D and E) mRNA levels of the CXC chemokines MIP-2 (D) and KC (E) in the cecal tissue as determined by RT-qPCR. Bars represent the geometric mean \pm standard error. ns, not statistically significant.

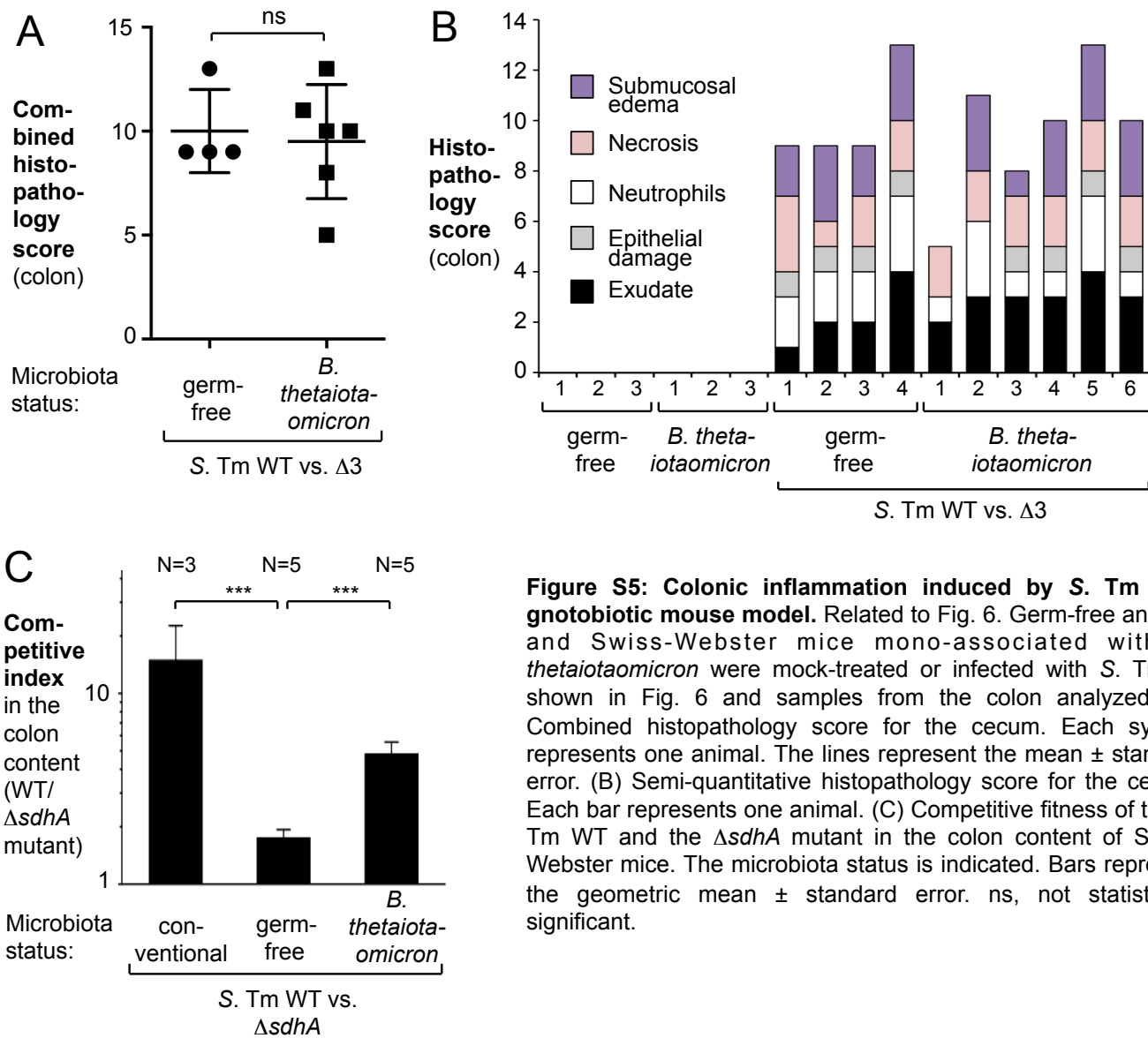


Figure S5: Colonic inflammation induced by *S. Tm* in a gnotobiotic mouse model. Related to Fig. 6. Germ-free animals and Swiss-Webster mice mono-associated with *B. thetaiotaomicron* were mock-treated or infected with *S. Tm* as shown in Fig. 6 and samples from the colon analyzed. (A) Combined histopathology score for the cecum. Each symbol represents one animal. The lines represent the mean \pm standard error. (B) Semi-quantitative histopathology score for the cecum. Each bar represents one animal. (C) Competitive fitness of the *S. Tm* WT and the $\Delta sdhA$ mutant in the colon content of Swiss-Webster mice. The microbiota status is indicated. Bars represent the geometric mean \pm standard error. ns, not statistically significant.

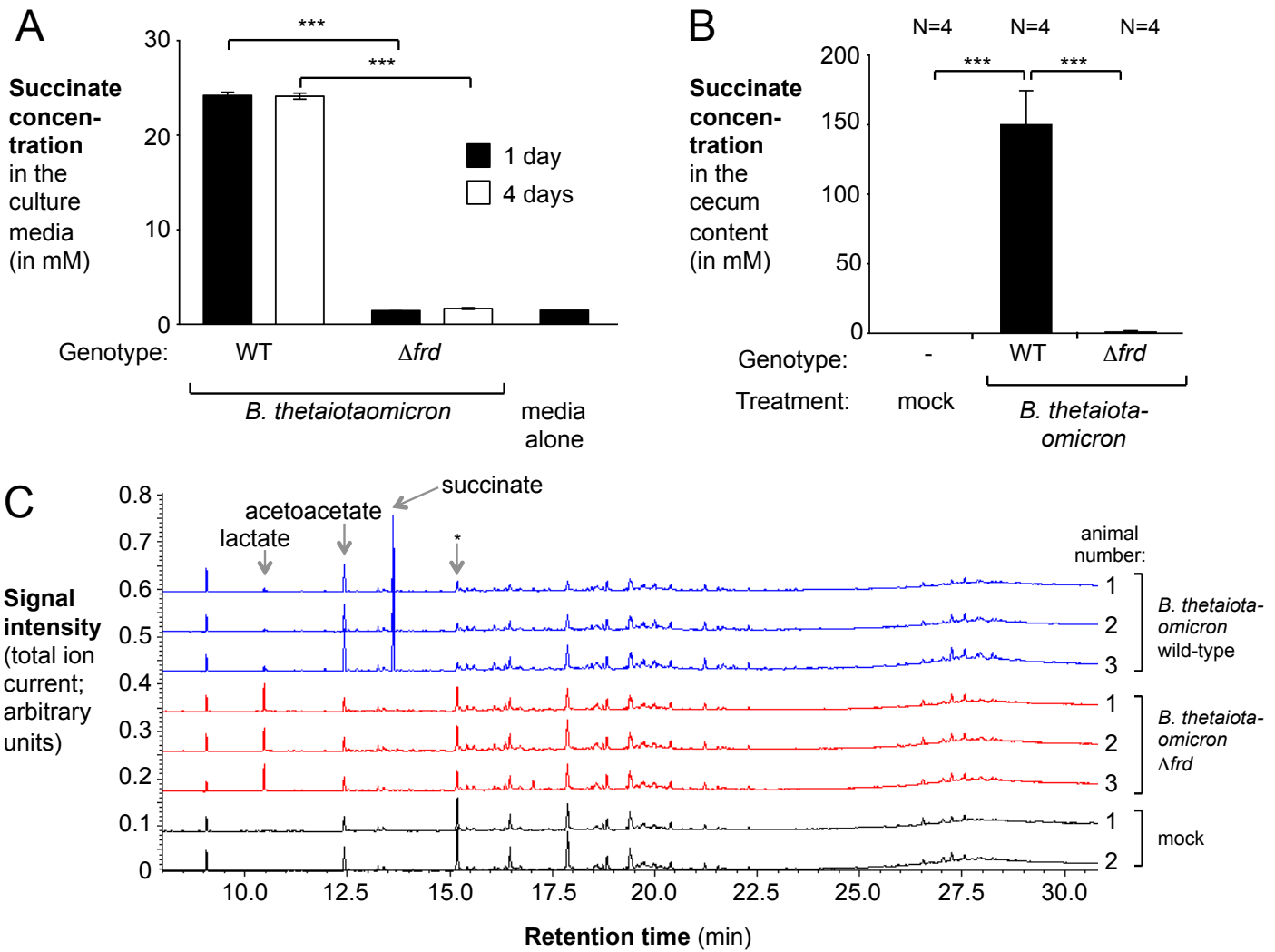


Figure S6: Succinate measurement and metabolite profiling in gnotobiotic mice. Related to Fig. 6. (A) The *B. thetaiotaomicron* wild-type strain (WT) and the $\Delta frdCAB$ (Δfrd) mutant were cultured under anaerobic conditions in modified TYG broth for 1 (black bars) or 4 days (white bars). The concentration of succinate in the culture supernatant was quantified by GC/MS/MS. Bars represent the geometric mean \pm standard error from 4 independent experiments. (B and C) Germ-free animals were mono-associated with the *B. thetaiotaomicron* wild-type strain (WT), the $\Delta frdCAB$ (Δfrd), or were mock-treated. (B) The concentration of succinate was determined using GC/MS/MS. (C) The metabolite profile in the cecal content was determined by GC/MS using a platform tailored towards discovery of simple sugars, amino acids, and carboxylic acids. Four animals per group were analyzed, of which 2-3 representative examples are shown. Metabolites that differed in abundance between the samples are identified using gray arrows. Star (*) denotes a reagent peak.

Supplemental Table 1: Primers used in this study. Related to the description of plasmid construction, quantification of inflammatory markers by RT-qPCR and bacterial gene expression in the methods details.

Targeted mutagenesis and complementation constructs		
Purpose	Sequence (restriction enzyme sites are shown in italics, sequences homologous to target genes are underlined)	Reference
Deletion of <i>sdhA</i>	5'-GCCATCTCCTTGCATG <u>GCGGGC</u> ATC <u>CTTACCGCGC</u> -3' 5'-GAAT <u>CTTCGTT</u> ACAC <u>ACCCCACACCACAAAC</u> -3' 5'-GGTGTGTA <u>ACGAAGATT</u> CGTACTTATTAAATTGC-3' 5'-CAAGGAATGGTGCATGC <u>ACTGACGCAGTCATAATG</u> -3'	This study
Deletion of <i>sucAB</i>	5'-GGAT <u>CCCCGT</u> CATT <u>CTGGTGG</u> -3' 5'-CCG <u>TCTAGAT</u> TAAG <u>GCATCTTCTG</u> -3' 5'-CCT <u>CTAGAT</u> CAG <u>CAAGAGCATCACC</u> -3' 5'-GTC <u>GACCTGGTCACGCATT</u> CACG-3'	This study
Deletion of <i>sucCD</i>	5'-GGAT <u>CCTGAAAGCGGTAGTGG</u> -3' 5'-GCG <u>TCTAGAGT</u> GTT <u>CTGTCCATCC</u> -3' 5'-CCT <u>CTAGAAACTCGCTGTTCTGC</u> -3' 5'-GTC <u>GACTCTGCCAGGTTATCGC</u> -3'	This study
Deletion of <i>aceAB</i>	5'-GGAT <u>CCGCTATTGTCTGTTGGG</u> -3' 5'-CCG <u>TCTAGAGCCTGTGGATT</u> CATC-3' 5'-GGT <u>CTAGAGTTTGATTGATGCC</u> -3' 5'-GTC <u>GACTAAAACAAC</u> TCG <u>TTCGCC</u> -3'	This study
Deletion of <i>dcuA</i>	5'-GCCATCTCCTTGCAT <u>GTGATTGAGGCGACATCTG</u> -3' 5'-GGAT <u>GAAGACTTGTGTTAAC</u> A <u>AGTTGATATTAAATTG</u> -3'	This study

	5'-AACAAACAAGTCTTCATCCCAGGCACCCTGGG-3' 5'-CAAGGAATGGTGCATGCCAGCCGCCCTGGTT-3'		
Deletion of <i>dcuB</i>	5'-GCCATCTCCTTGCATGAGCCGGAACATTACTCTTAC-3' 5'-GCTGTGGTCGCGATAAACCCAGTCAATTTCG-3' 5'-TTATCGCGACCACAGCTCATTCTGCCGGTTG-3' 5'-CAAGGAATGGTGCATGCAGGCCGCGGTGCCAGC-3'	This study	
Deletion of <i>dctA</i>	5'-GCCATCTCCTTGCATGCCTGATGGTCACGGTGGG-3' 5'-TGGCGAGATGAAGTAAAACACAGGTCTTGTAAAG-3' 5'-TTTACTTCATCTGCCACTTATGCCCG-3' 5'-CAAGGAATGGTGCATGTCATAGAAAGCCTGAATTTCGGC-3'	This study	
Generation of pSW327	5'-CATGCGATATCGAGCTCGATGGAAACAAGCTGCTG-3' 5'-ATTCCCGGGAGAGCTACTAATGCCAGAAGTGTACC-3'	This study	
Compleme ntation of <i>sdhA</i>	5'-CTAGAGGTACCGCATGCTATTGCCTGATGGCGCT-3' 5'-AGCTCGATATCGCATGC GGTAACGACTTGATTAATTTCGAATTAG-3'	This study	
Deletion of <i>frdCAB</i>	5'-CGAATTCCCTGCAGCCCCGGGGGA TCCATTATTGACTGAAAAATGAAATAATAC-3' 5'-AAGCTCACGCAAATGATTG AATTAAATTATTAATTGTTAGAAC-3' 5'-TCAATCATTGCGTGAGCTGATTGATTAATAG-3' 5'-CGGCCGCTCTAGAACTAGTGG ATCCTTGTCAAGATACAATTGCTATGAC-3'	This study	
RT-qPCR			
Organism(s)	Target genes	Sequence	Reference
<i>Mus musculus</i>	<i>Gapdh</i>	5'-TGTAGACCATGTAGTTGAGGTCA-3'	(Overbergh)

		5'-AGGTCGGTGTGAACGGATTG-3'	et al., 2003)
<i>Mus musculus</i>	<i>Cxcl1 (Kc)</i>	5'-TGCACCCAAACCGAAGTCAT-3' 5'-TTGTCAGAACGCCAGCGTTCAC-3'	(Godinez et al., 2008)
<i>Mus musculus</i>	<i>Nos2</i>	5'-CCAGCCTTGCATCCTCATTGG-3' 5'-CCAAACACCAAGCTCATGCGG-3'	(Godinez et al., 2008)
<i>Mus musculus</i>	<i>Tnf</i>	5'-TTGGGTCTTGTTCACTCCACGG-3' 5'-CCTCTTCAGGTCACTTGGTAGG-3'	(Wilson et al., 2008)
S. Tm	16S rRNA	5'-TGTTGTGGTTAATAACCGCA-3' 5'-GACTACCAGGGTATCTAATCC-3'	(Barman et al., 2008)
S. Tm	<i>sucA</i>	5'-ATCCTGACTCGGTAGACGCT-3' 5'-AGTTGATCCGGTTGACTCC-3'	This study
S. Tm	<i>sdhA</i>	5'-GATGCTGTTGTGATTGGT-3' 5'-GGGAAGACTTCGAGAGCAG-3'	This study

Supplemental Table 2: Histopathology scoring. Scoring criteria for examination of H&E-stained cecal and colonic sections. Related to Fig. 4D, S1, S3, S4, and S5.

Score	Submucosal edema	Necrosis	Neutrophils	Epithelial damage	Exudate
0	Absent	Absent	0 - 5	Absent	Absent
1	Slight (<10%)	Slight necrosis	6 - 20	Desquamation	Slight accumulation
2	Mild (10%-20%)	Mild necrosis	21 - 50	Mild erosion	Mild accumulation
3	Moderate (20%-40%)	Moderate necrosis	51 - 100	Marked erosion	Moderate accumulation
4	Severe (>40%)	Severe necrosis	>100	Ulceration	Severe accumulation